Nat.Lab. Unclassified Report NL-UR 2002/823

Date of issue: August 2002

Introduction to and Usage of the Bipolar Transistor Model Mextram

J.C.J. Paasschens and R. v.d. Toorn

Unclassified report

©Koninklijke Philips Electronics N.V. 2002

Authors' address data: J.C.J. Paasschens WAY41; Jeroen.Paasschens@philips.com
R. v.d. Toorn WAY41; Ramses.van.der.Toorn@philips.com

©Koninklijke Philips Electronics N.V. 2002
All rights are reserved. Reproduction in whole or in part is
prohibited without the written consent of the copyright owner.

Unclassified Report: NL-UR 2002/823

Title: Introduction to and Usage of the Bipolar Transistor Model Mextram

Author(s): J.C.J. Paasschens and R. v.d. Toorn

Part of project: Compact modelling

Customer: Semiconductors

Keywords: Mextram, spice, equivalent circuits, analogue simulation, semiconductor device models, semiconductor device noise, nonlinear distortion, heterojunction bipolar transistors, bipolar transistors, integrated circuit modelling, semiconductor technology

Abstract: Mextram is a compact model for vertical bipolar transistors. For a designer such a compact model, together with the parameters for a specific technology, is the interface between the circuit design and the real transistor. To be able to use Mextram in an efficient way one needs an understanding of some of the basics of Mextram. This report is meant to give a desginer an introduction into Mextram, level 504.

In this report we describe Mextram 504. We discuss its equivalent circuit and how the various elements of this circuit are connected to the various regions of a real transistor. We discuss the similarities and differences of Mextram 504 and the well-known Spice-Gummel-Poon model. Then we sketch the effects that can play a role in the low-doped collector epilayer of a bipolar transistor and how these are modelled within Mextram 504.

We show how one can handle the substrate resistance/capacitance network, that is not an integral part of Mextram. Furthermore, we discuss the possibilities of modelling self heating and mutual heating with Mextram 504. At last we show what information can be found from the operating point information that is supplied by many circuit simulators.

©Koninklijke Philips Electronics N.V. 2002

Preface

The Mextram bipolar transistor model has been put in the public domain in Januari 1994. At that time level 503.1 of Mextram was used within Koninklijke Philips Electronics N.V. In June 1995 level 503.2 was released which contained some improvements.

Mextram level 504 contains a complete review of the Mextram model. This document gives an introduction for designers.

August 2002, J.P.

History of model

January 1994 : Release of Mextram level 503.1

June 1995 : Release of Mextram level 503.2
- Improved description of Early voltage
- Improved description of cut-off frequency
- Parameter compatible with level 503.1

June 2000 : Release of Mextram level 504 (preliminary version)
- Complete review of the model

April 2001 : Release of Mextram level 504

Small fixes:
- Parameters R_{th} and C_{th} added to *MULT*-scaling
- Expression for α in operating point information fixed

Changes w.r.t. June 2000 version:
- Addition of overlap capacitances C_{BEO} and C_{BCO}
- Change in temperature scaling of diffusion voltages
- Change in neutral base recombination current
- Addition of numerical examples with self-heating

September 2001 : Mextram level 504.1

Lower bound on R_{th} is now 0°C/W

Small changes in F_{ex} and $Q_{B_1B_2}$ to enhance robustness

March 2002 : Changes in implementation for increased numerical stability

Numerical stability increased of x_i/W_{epi} at small $\mathcal{V}_{\mathrm{C_1C_2}}$

Numerical stability increased of p_0^*

 ©Koninklijke Philips Electronics N.V. 2002

Contents

Contents **v**

1 Introduction **1**

1.1 Notation 1

2 Explanation of the equivalent circuit **2**

2.1 General nature of the equivalent model 2

2.2 Intrinsic transistor and resistances 4

2.3 Extrinsic transistor and parasitics 5

2.4 Extended modelling 5

2.5 Overview of parameters 8

3 Mextram's formulations compared to Spice-Gummel-Poon **12**

3.1 General parameters 12

3.2 DC model 12

3.2.1 Main current and Early effect 12

3.2.2 Forward base current 15

3.2.3 Reverse base current 16

3.2.4 Avalanche current 17

3.2.5 Substrate currents 18

3.2.6 Emitter resistance 18

3.2.7 Base resistance 18

3.2.8 Collector resistance and epilayer model 19

3.3 AC model 19

3.3.1 Overlap capacitances 19

3.3.2 Depletion capacitances 20

3.3.3 Diffusion charges 21

3.3.4 Excess phase shift 22

3.4 Noise model 23

3.4.1 Thermal noise 23

3.4.2 Shot noise 23

3.4.3 Flicker noise 23

©Koninklijke Philips Electronics N.V. 2002

3.5 Self-heating 24
3.6 Temperature model 24
3.6.1 Resistances 24
3.6.2 Diffusion voltages 25
3.6.3 Saturation currents 25
3.6.4 Current gains 26
3.6.5 Other quantities 26
3.7 Geometric scaling 26

4 The collector epilayer model **27**
4.1 Introduction 27
4.2 Some qualitative remarks on the description of the epilayer 27

5 The substrate network **34**

6 Usage of (self)-heating with Mextram **36**
6.1 Dynamic heating 36
6.1.1 Self-heating 36
6.1.2 Mutual heating 38
6.1.3 Advantages 38
6.1.4 Disadvantages 38
6.2 Static heating 39
6.2.1 Advantages 39
6.2.2 Disadvantages 39
6.3 Combining static and dynamic heating 39
6.4 The thermal capacitance 41

7 Operating point information **42**
7.1 Approximate small-signal circuit 42
7.2 DC currents and charges 43
7.3 Elements of full small-signal circuit 44

References **47**

 ©Koninklijke Philips Electronics N.V. 2002

1 Introduction

Mextram [1, 2] is a compact model for vertical bipolar transistors. A compact transistor model tries to describe the I-V characteristics of a transistor in a compact way, such that the model equations can be implemented in a circuit simulator. In principle Mextram is the same kind of model as the well known Ebers-Moll [3] and (Spice)-Gummel-Poon [4] models, described for instance in the texts about general semiconductor physics, Refs. [5, 6], or in the texts dedicated to compact device modelling [7, 8, 9]. These two models are, however, not capable of describing many of the features of modern down-scaled transistors. Therefore one has extended these models to include more effects. One of these more extended models is Mextram, which in its earlier versions has already been discussed in for instance Refs. [8, 10].

The complete model definition of Mextram, level 504, can be found on the web-site [1], for instance in the report [2]. In that report a small introduction is given into the physical basics of all the equations. An extensive physical derivation of all the model equations is given in the report [11]. In both reports, however, the emphasis is not directly on the designer who has to use the model. In this report, therefore, we give excerpts from the reports above, as well as some new material, that should give a designer an idea of what Mextram is, and how it can be used in circuit simulation. Since the bipolar transistor model of Gummel and Poon [4] (or its Spice-implementation) is so well-known, we will assume that the Spice-Gummel-Poon model (SGP) is known, and we will refer to it.

In Chapter 2 we will start with discussing the equivalent circuit of Mextram. This enables us to give an overview of all the regions and the physical effects in those regions that Mextram is able to model. It also gives an overview of the parameters of Mextram. In Chapter 3 we will give the basic equations of Mextram and compare these, where possible to those of Spice-Gummel-Poon (SGP). In that way a designer with knowledge of SGP can see where the differences are, but also where many of the similarities between the models lie. Mextram has a few main differences with SGP. The first is the more extensive equivalent circuit, important for more accurate modelling of all kinds of RC-times. The second is the much more accurate modelling of the collector epilayer. An introduction into that is given in Chapter 4. Furthermore, Mextram contains a description of the parasitic PNP, and therefore has a substrate contact. A short note about the substrate network that should be added to Mextram is given in Chapter 5. At last, Mextram contains self-heating, whereas SGP does not. An introduction of how to use self-heating is given in Chapter 6. As a help to the designer most circuit simulators are capable of giving operating point information. The kind of information that is available is discussed in Chapter 7.

1.1 Notation

To improve the clarity of the different formulas we used different typographic fonts. For parameters we use a sans-serif font, e.g. $\mathsf{V}_{\mathsf{d}_\mathsf{E}}$ and R_{Cv}. A list of all parameters is given in Chapter 2. For the node-voltages as given by the circuit simulator we use a calligraphic $\mathcal{V}$, e.g. $\mathcal{V}_{\mathrm{B_2E_1}}$ and $\mathcal{V}_{\mathrm{B_2C_2}}$. All other quantities are in normal (italic) font, like I_f and q_B.

©Koninklijke Philips Electronics N.V. 2002

2 Explanation of the equivalent circuit

2.1 General nature of the equivalent model

The description of a compact bipolar transistor model is based on the physics of a bipolar transistor. An important part of this is realizing that a bipolar transistor contains various regions, all with different doping levels. Schematically this is shown in Fig. 1. In this report we will base our description on a NPN transistor. It might be clear that the same model can be used for PNP transistors, using equivalent formulations. One can discern the emitter, the base, collector and substrate regions, as well as an intrinsic part and an extrinsic part of the transistor.

One of the steps in developing a compact model of a bipolar transistor is the creation of an equivalent circuit. In such a circuit the different regions of the transistor are modelled with their own elements. In Fig. 1 we have shown a simplified version of the Mextram equivalent circuit, in which we only show the intrinsic part of the transistor, as well as the resistances to the contacts. This simplified circuit is comparable to the Gummel-Poon equivalent circuit.

The circuit has a number of internal nodes and some external nodes. The external nodes are the points where the transistor is connected to the rest of the world. In our case these are the collector node C, the base node B and the emitter node E. The substrate node S is not shown yet since it is only connected to the intrinsic transistor via parasitics which we will discuss later. Also five internal nodes are shown. These internal nodes are used to define the internal state of the transistor, via the local biases. The various elements that connect the internal and external nodes can then describe the currents and charges in the corresponding regions. These elements are shown as resistances, capacitances, diodes and current sources. It is, however, important to note that most of these elementary elements are not the normal linear elements one is used to. In a compact model they describe in general non-linear resistances, non-linear charges and non-linear current sources (diodes are of course non-linear also). Furthermore, elements can depend on voltages on other nodes than those to which they are connected.

For the description of all the elements we use equations. Together all these equations give a set of non-linear equations which will be solved by the simulator. In the equations a number of parameters are used. The equations are the same for all transistors. The value of the parameters will depend on the specific transistor being modelled. We will give an overview of the parameters of Mextram 504 in the next section. For a compact model it is important that these parameters can be extracted from measurements on real transistors. For Mextram 504 this is described in a separate report [12]. This means that the number of parameters can not be too large. On the other hand, many parameters are needed to describe the many different transistors in all regimes of operation.

 ©Koninklijke Philips Electronics N.V. 2002

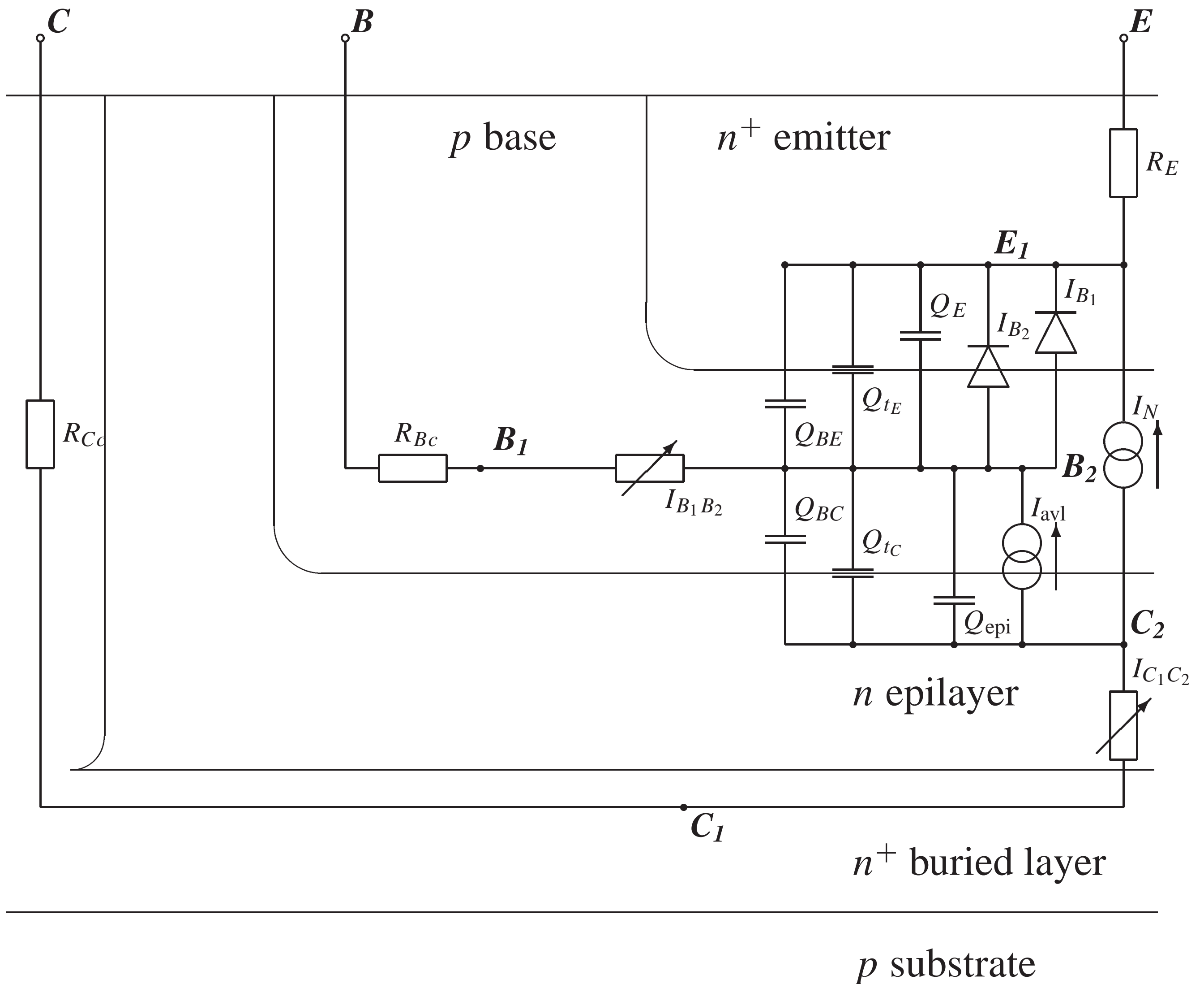

Figure 1: *A schematic cross-section of a bipolar transistor is shown, consisting of the emitter, base, collector and substrate. Over this cross-section we have given a simplified equivalent circuit representation of the Mextram model, which doesn't have the parasitics like the parasitic PNP, the base-emitter sidewall components, and the overlap capacitances. We did show the resistances from the intrinsic transistor to the external contacts. The current* $I_{B_1B_2}$ *describes the variable base resistance and is therefore sometimes called* R_{Bv}*. The current* $I_{C_1C_2}$ *describes the variable collector resistance (or epilayer resistance) and is therefore sometimes called* R_{Cv}*. This equivalent circuit is similar to that of the Gummel-Poon model, although we have split the base and collector resistance into two parts.*

©Koninklijke Philips Electronics N.V. 2002

2.2 Intrinsic transistor and resistances

Let us now discuss the various elements in the simplified circuit. The precise expressions will be given in the following chapters. Here we will only give a basic idea of the various elements in the Mextram model. Let us start with the resistances. Node E_1 corresponds to the emitter of the intrinsic transistor. It is connected to the external emitter node via the emitter resistor R_E. Both the collector node C and the base node B are connected to their respective internal nodes B_2 and C_2 via two resistances. For the base these are the constant resistor R_{Bc} and the variable resistor R_{Bv}. This latter resistor, or rather this non-linear current source, describes DC current crowding under the emitter. Between these two base resistors an extra internal node is present: B_1. The collector also has a constant resistor R_{Cc} connected to the external collector node C. Furthermore, since the epilayer is lightly doped it has its own 'resistance'. For low currents this resistance is R_{Cv}. For higher currents many extra effects take place in the epilayer. In Mextram the epilayer is modelled by a controlled current source $I_{C_1C_2}$.

Next we discuss the currents present in the model. First of all the main current I_N gives the basic transistor current. In Mextram the description of this current is based on the Gummel's charge control relation [13], see also [11]. This means that the deviations from an ideal transistor current are given in terms of the charges in the intrinsic transistor. The main current depends (even in the ideal case) on the voltages of the internal nodes E_1, B_2 and C_2.

Apart from the main current we also have base currents. In the forward mode these are the ideal base current I_{B_1} and the non-ideal base current I_{B_2}. Since these base currents are basically diode currents they are represented by a diode in the equivalent circuit.

In reverse mode Mextram also has an ideal and a non-ideal base current. However, these are mainly determined by the extrinsic base-collector pn-junction. Hence they are not included in the intrinsic transistor. The last current source in the intrinsic transistor is the avalanche current. This current describes the generation of electrons and holes in the collector epi-layer due to impact ionisation, and is therefore proportional to the current $I_{C_1C_2}$. We only take weak avalanche into account.

At last the intrinsic transistor shows some charges. These are represented in the circuit by capacitances. The charges Q_{t_E} and Q_{t_C} are almost ideal depletion charges resulting from the base-emitter and base-collector pn-junctions. The extrinsic regions will have similar depletion capacitances. The two diffusion charges Q_{BE} and Q_{BC} are related to the built-up of charge in the base due to the main current: the main current consists of mainly electrons traversing the base and hence adding to the total charge. Q_{BE} is related to forward operation and Q_{BC} to reverse operation. In hard saturation both are present. The charge Q_E is related to the built-up of holes in the emitter. Its bias dependence is similar to that of Q_{BE}. The charge Q_{epi} describes the built-up of charge in the collector epilayer.

 ©Koninklijke Philips Electronics N.V. 2002

2.3 Extrinsic transistor and parasitics

After the description of the intrinsic transistor we now turn to the extrinsic PNP-region and the parasitics. In Fig. 2 we have added some extra elements: a base-emitter side-wall parasitic, the extrinsic base-collector regions, the substrate and the overlap capacitances. Note that Mextram has a few flags that turn a part of the modelling on or off. In Fig. 3 on page 7, where it is easily found for reference, the full Mextram equivalent circuit is shown which also includes elements only present when all the extended modelling is used.

Let us start with the base-emitter sidewall parasitic. Since the pn-junction between base and emitter is not only present in the intrinsic region below the emitter, a part of the ideal base current will flow through the sidewall. This part is given by $I_{B_1}^S$. Similarly, the sidewall has a depletion capacitance given by the charge $Q_{t_E}^S$.

The extrinsic base-collector region has the same elements as the intrinsic transistor. We already mentioned the base currents. For the base-collector region these are the ideal base current I_{ex} and the non-ideal base current I_{B_3}. Directly connected to these currents is the diffusion charge Q_{ex}. The depletion capacitance between the base and the collector is split up in three parts. We have already seen the charge Q_{t_C} of the intrinsic transistor. The charge Q_{tex} is the junction charge between the base and the epilayer. Mextram models also the charge XQ_{tex} between the outer part of the base and the collector plug.

Then we have the substrate. The collector-substrate junction has, as any pn-junction, a depletion capacitance given by the charge Q_{t_S}. Furthermore, the base, collector and substrate together form a parasitic PNP transistor. This transistor has a main current of itself, given by I_{sub}. This current runs from the base to the substrate. The reverse mode of this parasitic transistor is not really modelled, since it is assumed that the potential of the substrate is the lowest in the whole circuit. However, to give a signal when this is no longer true a substrate failure current I_{Sf} is included that has no other function than to warn a designer that the substrate is at a wrong potential.

Finally the overlap capacitances C_{BEO} and C_{BCO} are shown that model the constant capacitances between base and emitter or base and collector, due to for instance overlapping metal layers (this should *not* include the interconnect capacitances).

2.4 Extended modelling

In Mextram two flags can introduce extra elements in the equivalent circuit (see Fig. 3 on page 7). When $\mathit{EXPHI} = 1$ the charge due to AC-current crowding in the pinched base (i.e. under the emitter) is modelled with $Q_{B_1B_2}$. (Also another non-quasi-static effect, base-charge partitioning, is then modelled.) When $\mathit{EXMOD} = 1$ the external region is modelled in some more detail (at the cost of some loss in the convergence properties in a circuit simulator). The currents I_{ex} and I_{sub} and the charge Q_{ex} are split in two parts, similar to the splitting of Q_{tex}. The newly introduced elements are parallel to the charge Q_{tex}.

©Koninklijke Philips Electronics N.V. 2002

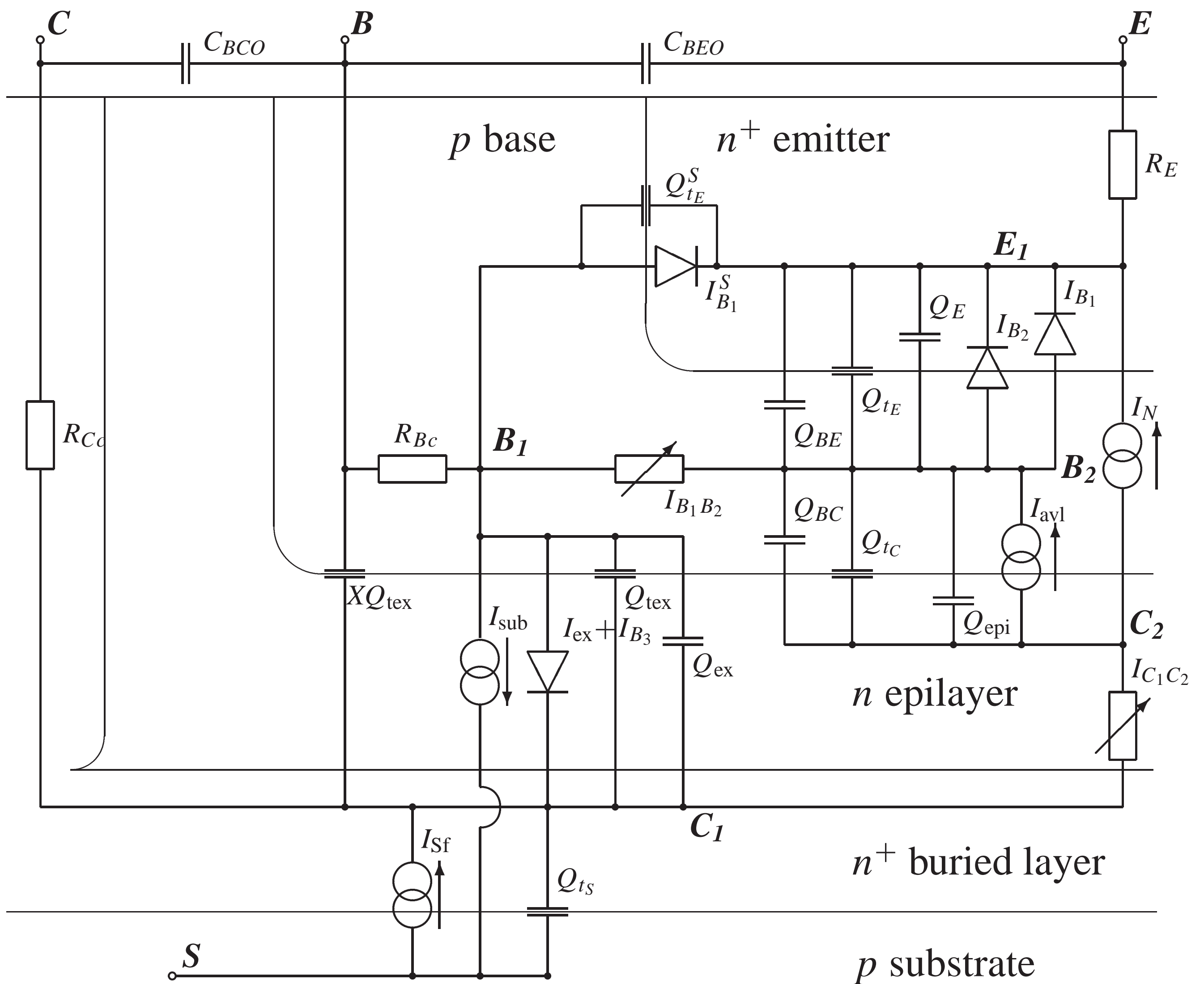

Figure 2: *Shown is the Mextram equivalent circuit for the vertical NPN transistor, without extra modelling (i.e.* EXMOD $= 0$ *and* EXPHI $= 0$*). As in Fig. 1 we have schematically shown the different regions of the physical transistor.*

 ©Koninklijke Philips Electronics N.V. 2002

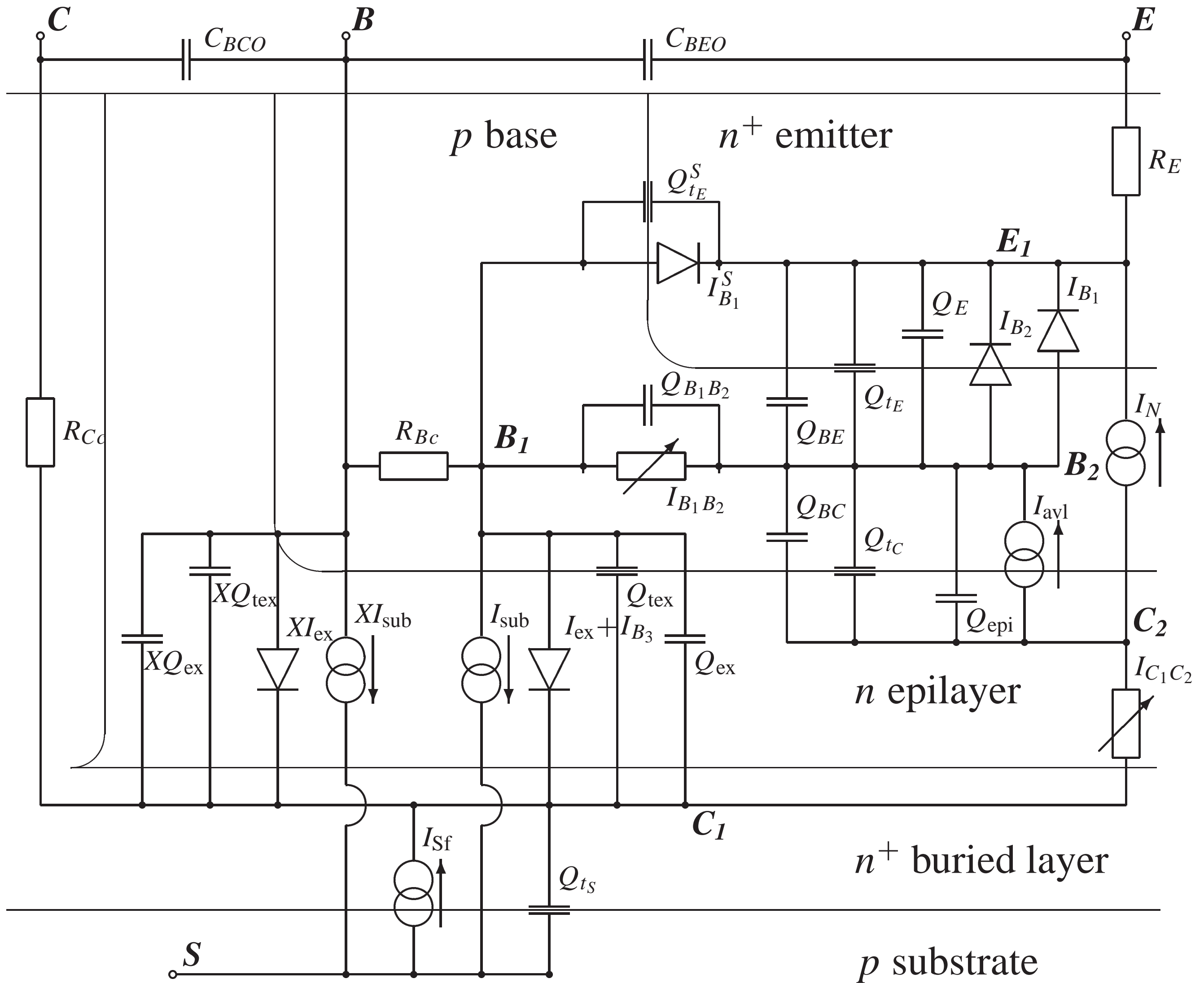

Figure 3: *The full Mextram equivalent circuit for the vertical NPN transistor. Schematically the different regions of the physical transistor are shown. The current* $I_{B_1B_2}$ *describes the variable base resistance and is therefore sometimes called* R_{Bv}*. The current* $I_{C_1C_2}$ *describes the variable collector resistance (or epilayer resistance) and is therefore sometimes called* R_{Cv}*. The extra circuit for self-heating is discussed in Chapter 6.*

©Koninklijke Philips Electronics N.V. 2002

2.5 Overview of parameters

In this section we will give an overview of the parameters used in Mextram. These parameters can be divided into different categories. In the formal description these parameters are given by a letter combination, e.g. IS. In equations however we will use a different notation for clarity, e.g. I_S. Note that we used a sans-serif font for this. Using this notation it is always clear in an equation which quantities are parameters, and which are not. Many of the parameters are dependent on temperature. For this dependence the model contains som extra parameters. When the parameter is corrected for temperature it is denoted by an index T, e.g. I_{ST}. In the formal documentation [1, 2] the difference between the parameter at reference temperature I_S and the parameter after temperature scaling I_{ST} is made in a very stringent way. In this report however we don't add the temperature subscript, unless it is needed.

First of all we have some general parameters. Flags are either 0 when the extra modelling is not used, or 1 when it is.

LEVEL	LEVEL	Model level, here always 504
EXMOD	EXMOD	Flag for EXtended MODelling of the external regions
EXPHI	EXPHI	Flag for extended modelling of distributed HF effects in transients
EXAVL	EXAVL	Flag for EXtended modelling of AVaLanche currents
MULT	MULT	Number of parallel transistors modelled together

As mentioned in the description of the equivalent circuit some currents and charges are split, e.g. in an intrinsic part and an extrinsic part. Such a splitting needs a parameter. There are 2 for the side-wall of the base-emitter junction. Then the collector-base region is split into 3 parts, using 2 parameters.

XI_{B_1}	XIBI	Fraction of the ideal base current that goes through the sidewall
XC_{j_E}	XCJE	Fraction of the emitter-base depletion capacitance that belongs to the sidewall
XC_{j_C}	XCJC	Fraction of the collector-base depletion capacitance that is under the emitter
X_{ext}	XEXT	Fraction of external charges/currents between B and C_1 instead of B_1 and C_1

A transistor model must in the first place describe the currents, and we use some parameters for this. The main currents of both the intrinsic and parasitic transistors are described by a saturation current and a high-injection knee current. We also have two Early voltages for the Early effect in the intrinsic transistor. The two ideal base currents are related to the main currents by a current gain factor. The non-ideal base currents are described by a saturation current and non-ideality factor or a cross-over voltage (due to a kind of high-injection effect). The avalanche current is described by three parameters.

 ©Koninklijke Philips Electronics N.V. 2002

I_s	IS	Saturation current for intrinsic transistor
I_k	IK	High-injection knee current for intrinsic transistor
I_{Ss}	ISS	Saturation current for parasitic PNP transistor
I_{ks}	IKS	High-injection knee current for parasitic PNP transistor
V_{ef}	VEF	Forward Early voltage of the intrinsic transistor
V_{er}	VER	Reverse Early voltage of the intrinsic transistor
β_f	BF	Current gain of ideal forward base current
β_{ri}	BRI	Current gain of ideal reverse base current
I_{Bf}	IBF	Saturation current of the non-ideal forward base current
m_{Lf}	MLF	Non-ideality factor of the non-ideal forward base current
I_{Br}	IBR	Saturation current of the non-ideal reverse base current
V_{Lr}	VLR	Cross-over voltage of the non-ideal reverse base current
W_{avl}	WAVL	Effective width of the epilayer for the avalanche current
V_{avl}	VAVL	Voltage describing the curvature of the avalanche current
S_{fh}	SFH	Spreading factor for the avalanche current

Mextram contains both constant and variable resistances. For variable resistances the resistance for low currents is used as a parameter. The epilayer resistance has two extra parameters related to velocity saturation and one smoothing parameter.

R_E	RE	Constant resistance at the external emitter
R_{Bc}	RBC	Constant resistance at the external base
R_{Bv}	RBV	Low current resistance of the pinched base (i.e. under the emitter)
R_{Cc}	RCC	Constant resistance at the external collector
R_{Cv}	RCV	Low current resistance of the epilayer
SCR_{Cv}	SCRCV	Space charge resistance of the epilayer
I_{hc}	IHC	Critical current for hot carriers in the epilayer
a_{xi}	AXI	Smoothing parameter for the epilayer model

All depletion capacitances are given in terms of the capacitance at zero bias, a built-in or diffusion voltage and a grading coefficient (typically between the theoretical values 1/2 for an abrupt junction and 1/3 for a graded junction). The collector depletion capacitance is limited by the width of the epilayer region. Its intrinsic part also has a current modulation parameter.

C_{j_E}	CJE	Depletion capacitance at zero bias for emitter-base junction
p_E	PE	Grading coefficient of the emitter-base depletion capacitance
V_{d_E}	VDE	Built-in diffusion voltage emitter-base
C_{j_C}	CJC	Depletion capacitance at zero bias for collector-base junction
p_C	PC	Grading coefficient of the collector-base depletion capacitance
V_{d_C}	VDC	Built-in diffusion voltage collector-base
X_p	XP	Fraction of the collector-base depletion capacitance that is constant

©Koninklijke Philips Electronics N.V. 2002

m_C	MC	Current modulation factor for the collector depletion charge
C_{j_S}	CJS	Depletion capacitance at zero bias for collector-substrate junction
p_S	PS	Grading coefficient of the collector-substrate depletion capacitance
V_{d_S}	VDS	Built-in diffusion voltage collector-substrate

New in Mextram 504 are two constant overlap capacitances.

C_{BEO}	CBEO	Base-emitter overlap capacitance
C_{BCO}	CBCO	Base-collector overlap capacitance

Most of the diffusion charges can be given in terms of the DC parameters. For accurate AC-modelling, however, it is better that DC effects and AC effects have their own parameters, which in this case are transit time parameters.

τ_E	TAUE	(Minimum) transit time of the emitter charge
m_τ	MTAU	Non-ideality factor of the emitter charge
τ_B	TAUB	Transit time of the base
τ_{epi}	TEPI	Transit time of the collector epilayer
τ_R	TAUR	Reverse transit time

Noise in the transistor is modelled by using only three extra parameters.

K_f	KF	Flicker-noise coefficient of the ideal base current
K_{fN}	KFN	Flicker-noise coefficient of the non-ideal base current
A_f	AF	Flicker-noise exponent

Then we have the temperature parameters. First of all two parameters describe the temperature itself. Next we have some temperature coefficients, that are related to the mobility exponents in the various regions. We also need some bandgap voltages to describe the temperature dependence of some parameters.

T_{ref}	TREF	Reference temperature
dT_a	DTA	Difference between local ambient and global ambient temperatures
$A_{Q_{B0}}$	AQBO	Temperature coefficient of zero bias base charge
A_E	AE	Temperature coefficient of R_E
A_B	AB	Temperature coefficient of R_{Bv}
A_{epi}	AEPI	Temperature coefficient of R_{Cv}
A_{ex}	AEX	Temperature coefficient of R_{Bc}
A_C	AC	Temperature coefficient of R_{Cc}
A_S	AS	Temperature coefficient of the mobility related to the substrate currents

 ©Koninklijke Philips Electronics N.V. 2002

$dV_{g\beta f}$	DVGBF	Difference in bandgap voltage for forward current gain
$dV_{g\beta r}$	DVGBR	Difference in bandgap voltage for reverse current gain
V_{g_B}	VGB	Bandgap voltage of the base
V_{g_C}	VGC	Bandgap voltage of the collector
V_{g_S}	VGS	Bandgap voltage of the substrate
V_{g_j}	VGJ	Bandgap voltage of base-emitter junction recombination
$dV_{g\tau_E}$	DVGTE	Difference in bandgap voltage for emitter charge

New in Mextram 504 are two formulations that are dedicated to SiGe modelling. For a graded Ge content we have a bandgap difference. For recombination in the base we have another parameter.

dE_g	DEG	Bandgap difference over the base
X_{rec}	XREC	Pre-factor for the amount of base recombination

Also new in Mextram 504 is the description of self-heating, for which we have the two standard parameters.

R_{th}	RTH	Thermal resistance
C_{th}	CTH	Thermal capacitance

3 Mextram's formulations compared to Spice-Gummel-Poon

In this chapter we will give a summary of the most important equations of Mextram. We will compare them, where possible, with those of Spice-Gummel-Poon (SGP), and note the differences and similarities:

Mextram formulation; SGP formulation.

In all the equations we will use the Mextram formulation on the left and the equivalent SGP formulation on the right. We will also give the equivalence between parameters if present. For clarity, our comparison is based on the Pstar SGP implementation (known as bipolar transistor model, level 2). Sometimes the same SGP parameter is known under different names. We will indicate this, for example, as T_{ref}/T_{amb}.

3.1 General parameters

Let us start with some general parameters.

Mextram	SGP	comments
$LEVEL$	$LEVEL$	Typical simulator dependent parameter.
$MULT$	$AREA/M$	Naming depends on simulator. In most if not all cases non-integer values are allowed.
T_{ref}	T_{ref}/T_{amb}	The reference temperature might vary in naming, but always has the same function.
DTA	DTA	The increase in local ambient temperature is not present in all simulators. See also Chapter 6.
$EXMOD$	—	In Mextram three parameters are used as explicit flags. In SGP only the electrical parameters can act as a flag, like I_{RB}.
$EXPHI$	—	
$EXAVL$	—	

3.2 DC model

3.2.1 Main current and Early effect

The forward part of the main current is in both models almost equal:

$$I_f = I_S\, e^{\mathcal{V}_{B_2E_1}/V_T}; \qquad I_f = I_S\, e^{\mathcal{V}_{B_1E_1}/N_F V_T}. \tag{3.1}$$

The main difference is the non-ideality in the SGP formulation. The non-ideality factor or emission coefficient N_F is not present in Mextram. Experience has learned that the emission coefficient for Si-based processes is not needed. Any non-ideality in the collector current is due to the reverse-Early effect and will be modelled via the normalised base charge.

 ©Koninklijke Philips Electronics N.V. 2002

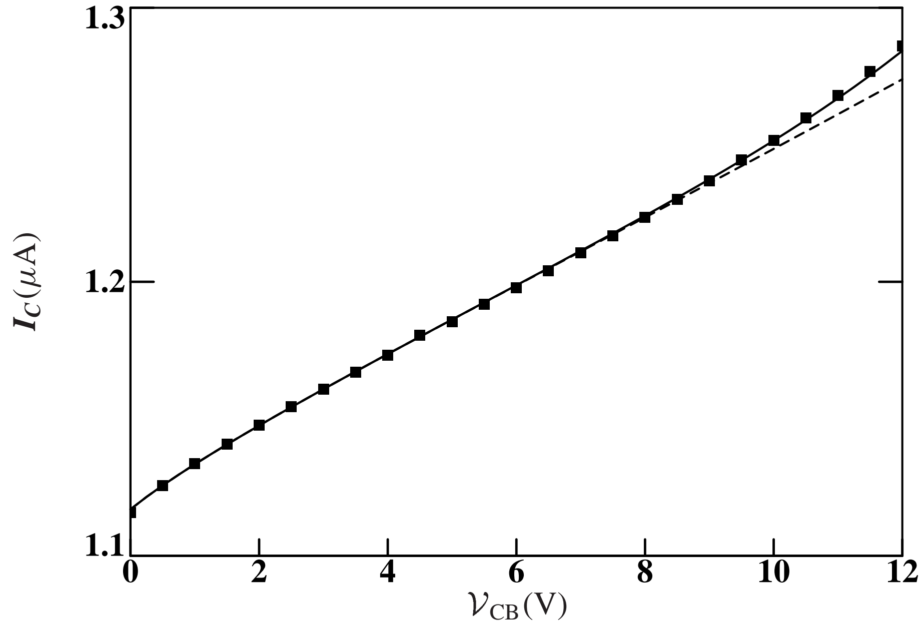

Figure 4: *Collector current as function of collector-base bias. The markers are from measurements. The solid line is the result of Mextram. The curvature in the current can clearly be observed. This curvature also means that the output conductance is not constant, as in SGP. The dashed lines is also from Mextram, but without avalanche.*

For the reverse main currents the same holds

$$I_r = I_S\, e^{\mathcal{V}_{B_2C_2}/V_T}; \qquad I_r = I_S\, e^{\mathcal{V}_{B_1C_1}/N_R V_T}. \tag{3.2}$$

Again the non-ideality factor is not present in Mextram.

The main current is now, in both cases

$$I_N = \frac{I_f - I_r}{q_B}; \qquad I_1 - I_2 = \frac{I_f - I_r}{q_B}. \tag{3.3}$$

The normalised base charge is something like

$$q_B = \frac{Q_{B0} + Q_{t_E} + Q_{t_C} + Q_{BE} + Q_{BC}}{Q_{B0}}, \tag{3.4}$$

where Q_{B0} is the base charge at zero bias. The total charge consists of Q_{B0}, the base-emitter and base-collector depletion charges and the base-emitter and base-collector diffusion charges. The normalised base charge can be given as a product of the Early effect (describing the variation of the base width given by the depletion charges) and a term which includes high injection effects. The Early effect term is in both models given using the normalised base charge $q_1 = 1 + Q_{t_E}/Q_{B0} + Q_{t_C}/Q_{B0}$, but in a different formulation:

$$q_1 = 1 + \frac{V_{t_E}}{V_{er}} + \frac{V_{t_C}}{V_{ef}}; \qquad q_1 = \left(1 - \frac{\mathcal{V}_{B_1E_1}}{V_{ar}} - \frac{\mathcal{V}_{B_1C_1}}{V_{af}}\right)^{-1}. \tag{3.5}$$

©Koninklijke Philips Electronics N.V. 2002

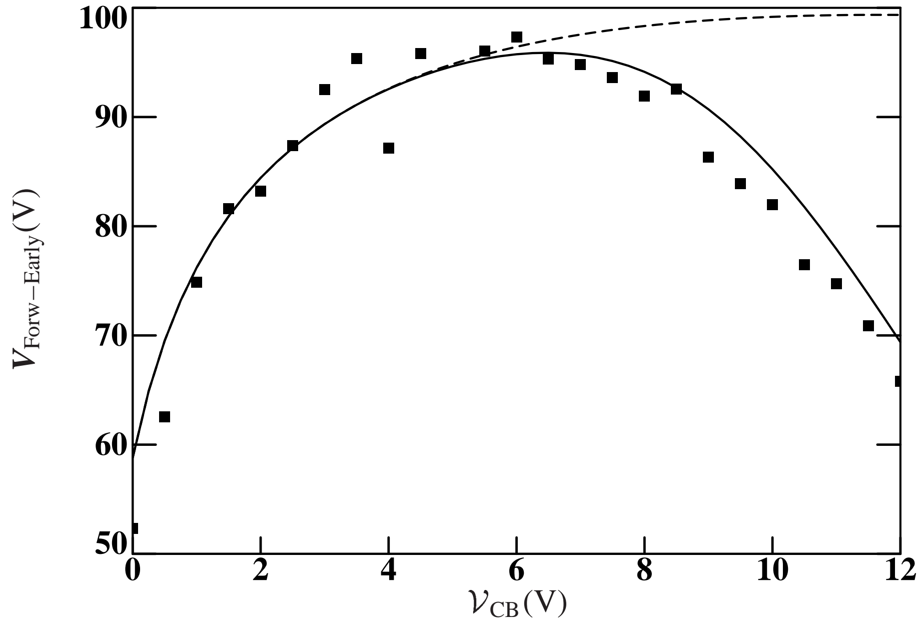

Figure 5: *The actual forward Early voltage obtained by numerical differentiation of the collector current in Fig. 4:* $V_{\mathrm{Forw-Early}} = I_C/(\mathrm{d}I_C/\mathrm{d}\mathcal{V}_{\mathrm{CB}})$. *SGP would give a constant value of this Early voltage. Again the dashed line is the Mextram result without avalanche.*

The voltages V_{t_E} and V_{t_C} describe the curvature of the depletion charges as function of junction biases, but not their magnitude: $Q_{t_E} = C_{jE} \cdot V_{t_E}$ and $Q_{t_C} = C_{jC} \cdot V_{t_C}$ (taking only the intrinsic parts into account). The difference in the Early effect modelling between SGP and Mextram is that Mextram includes the bias-dependence of the Early effect. Using the normalised depletion charges the actual Early voltage can be a function of current. Hence the collector current will not really be a straight line as function of collector bias, but it will show some curvature. This has been shown in Figs. 4 and 5. In SGP the Early effect is modelled by linearising the effect around zero bias.

Note that the Early voltage parameter here is only $V_{ef} = 44$ V. *So the parameter is much smaller than the actual Early voltage!*

Mextram is capable of modelling the effect of a gradient in the Ge-content in the base, as an extra option using the parameter dE_g [11, 14]. This will change the Early effects. This can mainly be seen in the sharp decrease of the current gain even before high-current effects (Webster effect, Kirk effect) start to play a role. We will not further discuss this here.

The influence of the diffusion charges on the current (Webster effect, giving a knee in the current) is modelled in the normalised base charge q_B as

$$q_B = q_1(1 + \tfrac{1}{2}n_0 + \tfrac{1}{2}n_B); \qquad q_B = q_1 \frac{\sqrt{1+4q_2}+1}{2}, \tag{3.6}$$

$$n_0 = \frac{4I_f/I_k}{1+\sqrt{1+4I_f/I_k}}; \qquad q_2 = \frac{I_f}{I_{KF}} + \frac{I_r}{I_{KR}}, \tag{3.7}$$

 ©Koninklijke Philips Electronics N.V. 2002

$$n_B = \frac{4I_r/I_k}{1+\sqrt{1+4I_r/I_k}}. \tag{3.8}$$

Although the formulations seem to be very different, the effect of both formulations is nearly the same. If one takes for instance $I_r = 0$ the results match. So the only difference is in the situation where I_f and I_r are both important. In SGP this is in hard-saturation. In Mextram the same happens in quasi-saturation. Since the latter regime is quite important in modern bipolar processes, Mextram gives a better result here.

I_s	I_s	Almost the same
—	N_F	Not needed in Mextram
—	N_R	Not needed in Mextram
V_{ef}	V_{af}	The forward Early voltages are present in both models. The Mextram value is, however, not close to the actual Early voltage, due to the bias-dependence. The Mextram value can be a factor 2 smaller.
V_{er}	V_{ar}	The reverse Early voltages are present in both models. The Mextram value is, however, not close to the actual Early voltage, due to the bias-dependence.
dE_g	—	Including a gradient in the Ge-content of the base is an extra option of Mextram.
I_k	I_{KF} & I_{KR}	Mextram contains only one knee current.

3.2.2 Forward base current

The forward base currents consist of an ideal part and a non-ideal part. Both parts are very similar to each other in the two models. For the ideal part we have

$$I_{B_1} = \frac{I_s}{\beta_f}\left(e^{\mathcal{V}_{B_2E_1}/V_T} - 1\right); \qquad I_{RE} = \frac{I_s}{\beta_f}\left(e^{\mathcal{V}_{B_1E_1}/V_T} - 1\right). \tag{3.9}$$

In Mextram the ideal forward base current can be split into a bottom and a sidewall component using the parameter XI_{B_1}. Mextram has an option to include the collector-voltage dependence of this base current, like in the case of neutral base recombination, using the parameter X_{rec} [11, 14].

Note that due to the reverse Early effect, shown for instance in Fig. 6, the actual current gain might be much smaller than the parameter value β_f! The current gain parameter β_f is the limit of the current gain for $\mathcal{V}_{BE}$ to zero, if there were no non-ideal base current. For the data of Fig. 6 we have $\beta_f \simeq 400$.

Also the non-ideal base current is almost the same in the two models

$$I_{B_2} = I_{Bf}\left(e^{\mathcal{V}_{B_2E_1}/m_{Lf}V_T} - 1\right); \qquad I_{LE} = I_{SE}\left(e^{\mathcal{V}_{B_1E_1}/N_E V_T} - 1\right). \tag{3.10}$$

©Koninklijke Philips Electronics N.V. 2002

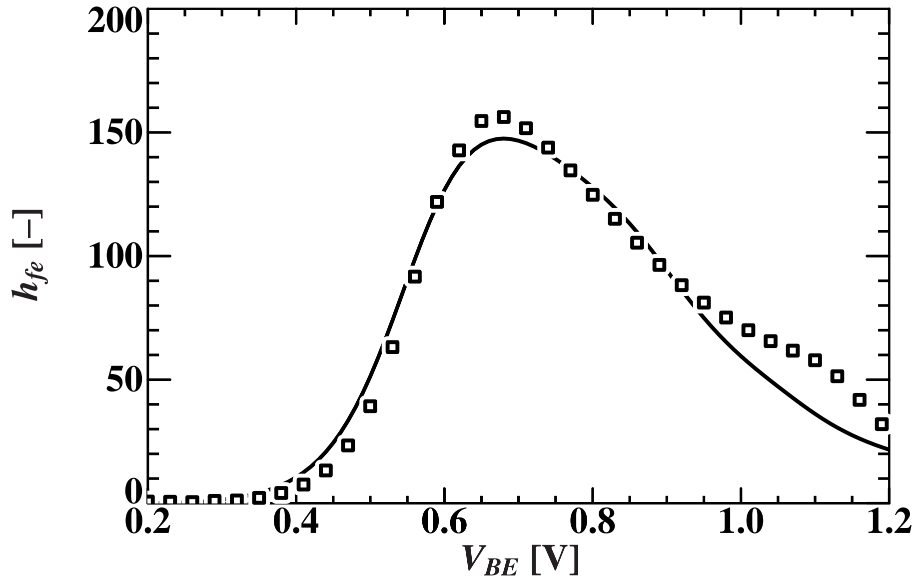

Figure 6: *The current gain as function of base-emitter voltage for a SiGe process which has a large reverse-Early effect (an effectively small reverse Early voltage). From Ref. [14].*

β_f	β_f	Almost the same
XI_{B_1}	—	No extra splitting of the base current is available in SGP.
X_{rec}	—	Neutral base recombination is an extra option of Mextram.
I_{Bf}	I_{SE}	The same
m_{Lf}	N_E	The same

3.2.3 Reverse base current

The reverse base currents are very similar to the forward base currents. For the ideal part in Mextram, however, the knee due to electrons injected in the base is the same as that of the main current. Note that in Mextram the reverse base current only exists in the extrinsic regions

$$I_{\mathrm{ex}} = \frac{I_s}{\beta_{ri}} \frac{2\left(e^{\mathcal{V}_{\mathrm{B_1C_1}}/V_T} - 1\right)}{1 + \sqrt{1 + I_s e^{\mathcal{V}_{\mathrm{B_1C_1}}/V_T}/I_k}}; \quad I_{RC} = \frac{I_s}{\beta_r}\left(e^{\mathcal{V}_{\mathrm{B_1C_1}}/V_T} - 1\right). \tag{3.11}$$

In Mextram the ideal reverse base current can be split into two extrinsic base currents, using X_{ext}. The same is done with the extrinsic capacitance, as we discuss later.

The non-ideal base current is somewhat different in both models. The SGP model contains a standard description of a non-ideal diode. Mextram contains a description based on SRH recombination where for small biases again a ideal slope exists. The cross-over from ideal

 ©Koninklijke Philips Electronics N.V. 2002

slope to non-ideal slope is determined by the cross-over voltage V_{Lr}.

$$I_{B_3} = I_{Br} \frac{e^{\mathcal{V}_{B_1C_1}/V_T} - 1}{e^{\mathcal{V}_{B_1C_1}/2V_T} + e^{V_{Lr}/2V_T}}; \qquad I_{LC} = I_{SC} \left(e^{\mathcal{V}_{B_1C_1}/N_C V_T} - 1 \right). \tag{3.12}$$

The two equations become the same in the very normal case of a low cross-over voltage V_{Lr} and a non-ideality factor of $N_C = 2$.

β_{ri}	β_r	Almost the same. Mextram contains a knee in the reverse base current. Furthermore, in Mextram β_{ri} only describes the intrinsic current gain, so not including substrate current effects.
I_{Br}	I_{SE}	The same
V_{Lr}	—	Mextram has a cross-over voltage,
—	N_E	where SGP has a non-ideality factor
X_{ext}	—	In Mextram splitting the extrinsic currents and charges is possible.

3.2.4 Avalanche current

Since SGP does not contain an avalanche model, we can not compare the models. In Mextram the avalanche current is given as

$$I_{\text{avl}} = I_{C_1C_2} \times G(\mathcal{V}_{B_1C_1}, I_{C_1C_2}) \tag{3.13}$$

where the generation factor, related to the multiplication factor $G = M - 1$, is a function of bias and current. It is supposed to be small ($G \ll 1$). For some results, see Figs. 4 and 5. Mextram is capable of modelling snapback effects at high currents, but only as an option.

In some SGP implementations an empirical model is present along the lines of

$$I_{\text{avl}} = I_{C_1C_2} \left(\frac{1}{1 - \left(\frac{\mathcal{V}_{C_1B_1}}{BV_{CBO}} \right)^N} - 1 \right). \tag{3.14}$$

Real breakdown is not modelled in Mextram. One of the most important reasons being that breakdown effects are really bad for convergence.

W_{avl}	—	No avalanche model present in SGP
V_{avl}	—	No avalanche model present in SGP
S_{fh}	—	No avalanche model present in SGP

3.2.5 Substrate currents

Mextram contains a substrate current, simply modelled as

$$I_{\mathrm{sub}} = \frac{2\, I_{Ss}\left(e^{\mathcal{V}_{\mathrm{B_1C_1}}/V_T} - 1\right)}{1 + \sqrt{1 + I_s e^{\mathcal{V}_{\mathrm{B_1C_1}}/V_T}/I_{ks}}}. \tag{3.15}$$

This substrate current describes the main current of the parasitic PNP, i.e. it describes the holes going from the base to the substrate. The current that runs in the case of a forward bias on the substrate-collector junction is not modelled in a physical way, since this should not happen anytime. There is only a signal current I_{Sf} to alert a designer to this wrong bias situation.

I_{Ss}	—	SGP has no substrate current
I_{ks}	—	SGP has no substrate current

3.2.6 Emitter resistance

The emitter resistance is in both models constant: R_E.

R_E	R_E	The same

3.2.7 Base resistance

The base resistance consists of a constant extrinsic part and a variable intrinsic part. Both Mextram and SGP contain both parts. In SGP, however, the two are lumped together into one resistance in the equivalent circuit.

The variable resistance in SGP can be due either to conductivity modulation (i.e. more charge in the base, modelled by q_B) or due to current crowding (modelled using the parameter I_{RB}). In Mextram both effects are taken into account simultaneously. The current crowding effect is based on the same theory as that of SGP [15, 16].

SGP models the variable part of the resistance as function of the current through it. This is done also in many publications about the subject. The problem then is that one has to decide whether the DC resistance or the small-signal resistance is taken. In Mextram the current through the resistance is modelled as function of the applied voltage. In that way both the DC resistance as well as the small-signal resistance follow directly form either I/V or $\mathrm{d}I/\mathrm{d}V$.

For the variable part we have in Mextram

$$I_{B_1B_2} = \frac{q_B}{3\, R_{Bv}}[2V_T(e^{\mathcal{V}_{\mathrm{B_1B_2}}/V_T}-1)+\mathcal{V}_{\mathrm{B_1B_2}}]. \tag{3.16}$$

 ©Koninklijke Philips Electronics N.V. 2002

It is important to realise that the actual intrinsic base resistance can be much smaller than R_{Bv}, due to current crowding, or, more likely, due to the extra charge in the base modelled by q_B!

For SGP we have either

$$I_{BB_1} = \frac{q_B}{R_B - R_{BM}} \mathcal{V}_{\mathrm{BB}_1}, \tag{3.17}$$

or

$$I_{BB_1} = \frac{f(I_{BB_1}, I_{RB})}{3\,(R_B - R_{BM})} \mathcal{V}_{\mathrm{BB}_1}. \tag{3.18}$$

R_{Bc}	R_{BM}	The extrinsic part of the base resistance is the same in both models: constant.
R_{Bv}	$R_B - R_{BM}$	Mextram has as parameter the zero-bias value of the intrinsic part. SGP has the zero-bias value of the total base resistance.
—	I_{RB}	Empirical parameter of SGP for a description of current crowding. Not needed in Mextram.

3.2.8 Collector resistance and epilayer model

The collector resistance not including the collector epilayer is in both models constant. SGP does not have a collector epilayer model for the current. (For the charges an empirical model is present.) It is this epilayer model which is maybe the largest improvement of Mextram over SGP. For this reason we discuss it in more detail in Chapter 4.

R_{Cc}	R_C	The same
R_{Cv}	—	SGP has no collector epilayer model
SCR_{Cv}	—	SGP has no collector epilayer model
I_{hc}	—	SGP has no collector epilayer model
a_{xi}	—	SGP has no collector epilayer model

3.3 AC model

3.3.1 Overlap capacitances

SGP has no overlap capacitances. Mextram has constant overlap capacitances. These are meant for modelling all kinds of constant parasitic capacitances that belong to the transistor. Most of them are vertical capacitances, say between poly layers or over STI, but also the effect of contacts is included. All interconnect capacitances are *not* included.

C_{BEO}	—	SGP has no overlap capacitances.
C_{BCO}	—	SGP has no overlap capacitances.

3.3.2 Depletion capacitances

The depletion capacitances of Mextram are not too different from those of SGP. The basic formulation is

$$C = \frac{C_j}{(1 - V/V_d)^p}. \tag{3.19}$$

Note that the notation of the parameters differs. Furthermore, in both models not the capacitance, but the charge is implemented.

There are a few differences, however.
• Mextram does not linearise the capacitances above a certain forward bias. It uses a smooth transition to a constant capacitance, for which no parameter is available. Since the transition in both models happens in the region where diffusion capacitances are dominant the difference in capacitance is not very important. For higher order derivatives, however, the SGP will give discontinuities.
• Mextram has a split in the base-emitter capacitance and an extra split in the base-collector capacitance. Having the extra nodes and having these splits in the capacitances gives a more accurate RC network. This means a better description of RC-times and hence of the small-signal parameters (e.g. Y-parameters).
• Reach-through of the base-collector capacitance is modelled, such that the capacitance becomes constant for large reverse biases. The basic formulation is

$$C = \frac{(1 - X_p)C_{j_C}}{\left(1 - V/V_{d_C}\right)^{p_C}} + X_p C_{j_C}. \tag{3.20}$$

• The base-collector capacitance is current dependent. This is related to the finite velocity of the electrons in the depletion layer, see Chapter 4.

C_{j_E}	C_{j_E}	The same
V_{d_E}	V_{j_E}/P_E	The same, apart from notation
p_E	M_E	The same, apart from notation
C_{j_C}	C_{j_C}	The same
V_{d_C}	V_{j_C}/P_C	The same, apart from notation
p_C	M_C	The same, apart from notation
C_{j_S}	C_{j_S}	The same
V_{d_S}	V_{j_S}/P_S	The same, apart from notation
p_S	M_S	The same, apart from notation
XC_{j_C}	XC_{j_C}	The same

 ©Koninklijke Philips Electronics N.V. 2002

XC_{j_E}	XC_{j_E}	SGP does not contain a split in the base-emitter capacitance
X_{ext}	X_{ext}	SGP does not contain an extra split of the base-collector capacitance
X_p	—	SGP does not model reach-through.
m_C	—	Mextram has a current dependence in the base-collector capacitance.
—	F_C	Mextram does not linearise the capacitances. Instead it the capacitances level off smoothly. For this model-constants a_{j_E}, a_{j_C}, and a_{j_S} are used.

3.3.3 Diffusion charges

For the low-current transit time there is not a large difference between Mextram and SGP. Only, Mextram contains two contributions, one from the emitter charge and one from the base charge. The contribution from the base charge is

$$Q_{BE} = q_1 \tau_B I_f \frac{2}{1+\sqrt{1+4I_f/I_k}}; \qquad Q_{ED} = \frac{1}{q_1}\tau_{FF} I_f \frac{2}{1+\sqrt{1+4I_f/I_{kf}}}. \tag{3.21}$$

In the SGP formulation we neglected here the contribution of I_r, which is zero anyway in normal operation, even in quasi-saturation/Kirk effect. Note that also the Early effect (via q_1) is taken into account differently. In Mextram there is a second contribution from the charged stored in the emitter (or the neutral part of the base-emitter depletion layer), which does not have a knee, but does have a non-ideality factor

$$Q_E = \tau_E I_s e^{\mathcal{V}_{B_2E_1}/m_\tau V_T}. \tag{3.22}$$

For higher currents the models start to differ quite a lot. SGP models the increase in effective transit time due to base-widening/quasi-saturation/Kirk effect as

$$\tau_{FF} = \tau_F \left[1 + X_{TF} \left(\frac{I_f}{I_f + I_{TF}} \right)^2 e^{\mathcal{V}_{B_1C_1}/1.44 V_{TF}} \right]. \tag{3.23}$$

In Mextram there is a collector epilayer model with a finite voltage drop. As a result the bias over the intrinsic base-collector junction, $\mathcal{V}_{B_2C_2}$, can become forward biased, such that the reverse part of the main current, I_r, becomes comparable to the forward part I_f. This results in an extra charge in the base

$$Q_{BC} = q_1 \tau_B I_r \frac{2}{1+\sqrt{1+4I_r/I_k}}. \tag{3.24}$$

Furthermore, there will be a lot of charge in the collector epilayer, due to the base-widening

$$Q_{\text{epi}} \simeq \tau_{epi} \left(\frac{x_i}{W_{\text{epi}}} \right)^2 I_{\text{epi}}. \tag{3.25}$$

©Koninklijke Philips Electronics N.V. 2002

where x_i / W_{epi} is the size of the base widening or thickness of the injection region, compared to the epilayer thickness, and I_{epi} is the current through the epilayer, normally equal to the main collector current I_N. In hard saturation when the current vanishes but the base-collector junction is still in forward, the real expression for Q_{epi} is such that it still describes the large built-up of charge in the epilayer.

$\tau_E + \tau_B$	τ_F	The low-current transit time in Mextram contains both a contribution from the emitter diffusion charge, as well as from the base-diffusion charge.
m_τ	—	SGP does not have an emitter diffusion charge.
τ_{epi}	—	A parameter which belongs directly to the quasi-saturation charge in the epilayer is not present in SGP. The effect is modelled in another way.
—	X_{TF}	The effect of increasing transit time due to quasi-saturation is modelled in Mextram via the collector epilayer model. This increase depends very much on τ_{epi}, but also on a lot of other parameters. Maybe $\tau_F \cdot X_{TF}$ could be compared to τ_{epi}, in the kind of effect they have.
—	I_{TF} & V_{TF}	See X_{TF}. In practice I_{TF} should be of the same order as I_{hc}, and V_{TF} should be of the same order as $R_{Cv} I_{hc}$ or $SCR_{Cv} I_{hc}$.
τ_R	τ_R	The reverse transit times are almost equivalent. But note that in Mextram it is used only in the extrinsic regions.

3.3.4 Excess phase shift

Both SGP and Mextram model excess phase shift. The difference in modelling is, however, quite different. The first thing to realise is that the most important contribution to the excess phase shift does not come from the intrinsic model. Instead the extrinsic capacitances and resistances (mainly the base resistance, the base-collector capacitance and its split using the parameter X_{ext}) are much more important. Only when these are correct, it is useful to look at non-quasi-static effects in the intrinsic transistor that can also cause excess phase shift. Since Mextram has a much better equivalent circuit, the intrinsic excess phase shift gives only a marginal effect.

In Mextram the intrinsic excess phase shift is modelled using base-charge partitioning (and only when $EXPHI = 1$). This means that a part of the charge Q_{BE}, which is $\mathcal{V}_{\mathrm{B_2E_1}}$-driven, is not supplied totally by the emitter, but also partly by the collector. To this end the charges Q_{BE} and Q_{BC} are changed from their previously calculated values to

$$Q_{BC} \rightarrow \tfrac{1}{3}\, Q_{BE} + Q_{BC}, \qquad (3.26)$$

$$Q_{BE} \rightarrow \tfrac{2}{3}\, Q_{BE}. \qquad (3.27)$$

In SGP excess phase shift is implemented using a Bessel approximation. Calculations are

 ©Koninklijke Philips Electronics N.V. 2002

not done with $I_1 = I_f/q_B$, but with I_X, which is a solution of the differential equation

$$3\omega_0^2 I_1 = \frac{\mathrm{d}^2 I_X}{\mathrm{d}t^2} + 3\omega_0 \frac{\mathrm{d}I_x}{\mathrm{d}t} + 3\omega_0^2 I_X, \quad (3.28)$$

where $\omega_0 = 1/(T_{FF} \cdot P_{TF}\,\pi/180)$.

Mextram also models an extra effect in the lateral direction (AC current crowding). Again only when $EXPHI = 1$ a charge is added parallel to the intrinsic base resistance

$$Q_{B_1B_2} = \tfrac{1}{5}\, \mathcal{V}_{\mathrm{B_1B_2}} \, \left(C_{t_E} + C_{BE} + C_E\right). \quad (3.29)$$

—	P_{TF}	Excess phase shift within Mextram has no extra parameter (besides, say, the base resistances and X_{ext}), but Mextram does have a switch ($EXPHI$) to turn the model on or off.

3.4 Noise model

The noise models of Mextram and SGP do not differ very much. But Mextram has a larger equivalent circuit, and hence more currents/resistances and corresponding noise sources.

3.4.1 Thermal noise

All resistances have thermal noise, including the variable part of the base resistance. For the variable collector resistance, the epilayer model of Mextram, a more advanced model is used for the case of base-widening.

3.4.2 Shot noise

All diode-like currents have shot-noise. This includes the main current, the main substrate current (not present in SGP) and all (forward and reverse) base currents.

3.4.3 Flicker noise

All base currents also have flicker noise ($1/f$-noise), modelled with a pre-factor K_f and a power A_f. In Mextram the non-ideal forward base current has its own pre-factor K_{fN} and a fixed power 2.

A_f	A_f	The same
K_f	K_f	The same
K_{fN}	—	Not present in SGP

©Koninklijke Philips Electronics N.V. 2002

3.5 Self-heating

SGP does not contain self-heating. Mextram does. See Chapter 6.

R_{th}	—	SGP does not contain self-heating
C_{th}	—	SGP does not contain self-heating

3.6 Temperature model

SGP has only 3 temperature parameters, whereas Mextram has 14 in total. This means that various Mextram parameters will correspond to the same SGP parameter. For the temperature scaling, we first need some definitions:

$$T_K = TEMP + DTA + 273.15 + \mathcal{V}_{\rm dT}, \tag{3.30}$$
$$T_{RK} = T_{ref} + 273.15, \tag{3.31}$$
$$t_N = \frac{T_K}{T_{RK}}, \tag{3.32}$$
$$V_T = \left(\frac{k}{q}\right) T_K, \tag{3.33}$$
$$V_{T_R} = \left(\frac{k}{q}\right) T_{RK}, \tag{3.34}$$
$$\frac{1}{V_{\Delta T}} = \frac{1}{V_T} - \frac{1}{V_{T_R}}. \tag{3.35}$$

Here T_K is the actual temperature including self-heating (see Chapter 6).

3.6.1 Resistances

In SGP the resistances are constant over temperature. In Mextram they all have their own parameter that is linked to the temperature dependence of the mobility.

$$R_{ET} = R_E \, t_N^{A_E}, \tag{3.36}$$
$$R_{BvT} = R_{Bv} \, t_N^{A_B - A_{Q_{B0}}}, \tag{3.37}$$
$$R_{BcT} = R_{Bc} \, t_N^{A_{ex}}, \tag{3.38}$$
$$R_{CcT} = R_{Cc} \, t_N^{A_C}, \tag{3.39}$$
$$R_{CvT} = R_{Cv} \, t_N^{A_{epi}}. \tag{3.40}$$

The parameter $A_{Q_{B0}}$ is not related to a mobility, but is an effective parameter describing the temperature scaling of the zero-bias base charge.

 ©Koninklijke Philips Electronics N.V. 2002

A_E	—	SGP has no temperature scaling for resistances
A_B	—	SGP has no temperature scaling for resistances
A_{ex}	—	SGP has no temperature scaling for resistances
A_C	—	SGP has no temperature scaling for resistances
A_{epi}	—	SGP has no temperature scaling for resistances
$A_{Q_{B0}}$	—	SGP has no temperature scaling for zero bias base charge

3.6.2 Diffusion voltages

The equation for the diffusion voltages is basically the same.

$$V_{dT} = -3V_T \ln t_N + V_d t_N + (1 - t_N) V_g. \tag{3.41}$$

Only Mextram makes sure that they do not become negative. The important parameter for the temperature scaling of the diffusion voltages is the bandgap V_g. SGP has only one bandgap: E_g.

Once the temperature scaling of the diffusion voltages has been done, the depletion capacitances in Mextram scale basically as

$$C_{jT} = C_j \left(\frac{V_d}{V_{dT}} \right)^p. \tag{3.42}$$

where the grading coefficient p is used.

V_{g_B}	E_g	Used for base-emitter diffusion voltage
V_{g_C}	E_g	Used for base-collector diffusion voltage
V_{g_S}	E_g	Used for substrate-collector diffusion voltage

3.6.3 Saturation currents

The equation for the saturation current is also similar

$$I_{sT} = I_s \, t_N^{4-A_B-A_{Q_{B0}}} \, e^{-V_{g_B}/V_{\Delta T}}; \qquad I_{sT} = I_s \, t_N^{X_{ti}} \, e^{-E_g/V_{\Delta T}}. \tag{3.43}$$

The same bandgap as before is used. The power of the pre-factor is different.

For the saturation current of the forward non-ideal base current we have

$$I_{BfT} = I_{Bf} \, t_N^{(6-2m_{Lf})} \, e^{-V_{g_J}/m_{Lf} \, V_{\Delta T}}; \qquad I_{SET} = I_{SE} \, t_N^{X_{ti}-X_{tb}} \, e^{-E_g/N_E \, V_{\Delta T}}. \tag{3.44}$$

For the saturation current of the reverse non-ideal base current we have

$$I_{BrT} = I_{Br} \, t_N^2 \, e^{-V_{g_C}/2 \, V_{\Delta T}}; \qquad I_{SCT} = I_{SC} \, t_N^{X_{ti}-X_{tb}} \, e^{-E_g/N_C \, V_{\Delta T}}. \tag{3.45}$$

The saturation current of the substrate scales with temperature as

$$I_{SsT} = I_{Ss} \, t_N^{4-A_S} \, e^{-V_{g_S}/V_{\Delta T}}. \tag{3.46}$$

©Koninklijke Philips Electronics N.V. 2002

V_{g_B}	E_g	Used for collector saturation current
V_{g_J}	E_g	Used for forward non-ideal base current
V_{g_C}	E_g	Used for reverse non-ideal base current
(A_B)	X_{ti}	A_B and X_{ti} have kind of the same purpose in the temperature scaling of the collector saturation current
V_{g_S}	—	SGP has no substrate current
A_S	—	SGP has no substrate current

3.6.4 Current gains

The temperature modelling of the current gains is different. In SGP a simple power dependence is used. In Mextram the model uses the normally small difference in bandgap between either emitter and base or base and collector. This can be important in the case of SiGe transistors, where the bandgap difference can become larger.

$$\beta_{fT} = \beta_f \; t_N^{A_E - A_B - A_{Q_{B0}}} \; e^{-dV_{g\beta f}/V_{\Delta T}}; \quad \beta_{fT} = \beta_f \; t_N^{X_{tb}}, \tag{3.47}$$

$$\beta_{riT} = \beta_{ri} \; e^{-dV_{g\beta r}/V_{\Delta T}}; \quad \beta_{rT} = \beta_r \; t_N^{X_{tb}}. \tag{3.48}$$

$dV_{g\beta f}$	—	SGP uses X_{tb}
$dV_{g\beta r}$	—	SGP uses X_{tb}
—	X_{tb}	Mextram uses $dV_{g\beta f}$ and $dV_{g\beta r}$

3.6.5 Other quantities

Mextram contains also temperature scaling of the Early voltages, the transit times and the material constant for the avalanche model. Since SGP does not have any equivalents, these are not discussed here.

$dV_{g\tau E}$	—	Specially for the emitter transit time

3.7 Geometric scaling

Geometric scaling is not present in both models. In both cases, geometric scaling can and should be done in a pre-processing way. There are no fundamental differences between Mextram and SGP in this respect. The only difference is that Mextram has a more complete equivalent circuit and is therefore capable of somewhat more advanced geometric scaling [12].

 ©Koninklijke Philips Electronics N.V. 2002

4 The collector epilayer model

4.1 Introduction

The collector epilayer of a bipolar transistor is the most difficult part to model. The reason for this is that a number of effects play a role and act together. Since in Spice-Gummel-Poon a model for this epilayer is not present at all, this chapter is devoted to a short introduction of the physics that plays a role. We will restrict ourselves to modelling the epilayer in as far as it is part of the intrinsic transistor. The current $I_{\text{epi}} = I_{C_1C_2}$ through the epilayer is for low current densities mainly determined by the main current I_N. Hence the epilayer is a part of the transistor that is current driven. Since the dope concentration in the epilayer is in general small, high injection effects are important. In that case the epilayer will be (partly) flooded by holes and electrons. Even though then the main current and the epilayer current depend on each other and their equations become coupled, we will still consider the epilayer to be current driven, i.e. our model will have I_{epi} as a starting quantity.

The regions where no injection takes place can either be ohmic, which implies charge neutral, or depleted. In depletion regions the electric field is large and the electrons will therefore move with the saturation velocity. These electrons can be called hot carriers. The electrons will contribute to the charge. In case of large currents this moving charge becomes comparable to the dope, the net charge decreases, or even changes sign. The net charge has its influence on the electric field, which in its turn determines the velocity of the electrons: for low electric fields we have ohmic behaviour, for large electric fields the velocity of the electrons will be saturated.

All these effects determine the effective resistance of the epilayer. As is well known, the potential drop over the collector region can cause quasi-saturation. In that case the external base-collector bias is in reverse, which is normal in forward operation, but the internal junction is forward biased. Injection of holes into the epilayer then takes place. The charge in the epilayer and in the base-collector region depends on the carrier concentrations in the epilayer, and will increase significantly in the case of quasi-saturation.

The electric field in the epilayer is directly related to the base-collector depletion capacitance. The avalanche current is determined by the same electric field, and in particular by its maximum. Hence our description of the epilayer must also include a correct description of the electric field.

4.2 Some qualitative remarks on the description of the epilayer

Let us now concentrate on a one-dimensional model of the lightly doped epilayer. We assume the epilayer to be along the x-axis from $x = 0$ to $x = W_{\text{epi}}$, as has been schematically shown in Fig. 7. The base is then located at $x < 0$, while the highly doped collector region, the buried layer, is situated at $x > W_{\text{epi}}$. We assume a flat dope in the epilayer and an abrupt epi-collector junction for the derivation of our equations. In the final description of the model some factors have been generalised to account for non-ideal profiles. (Like,

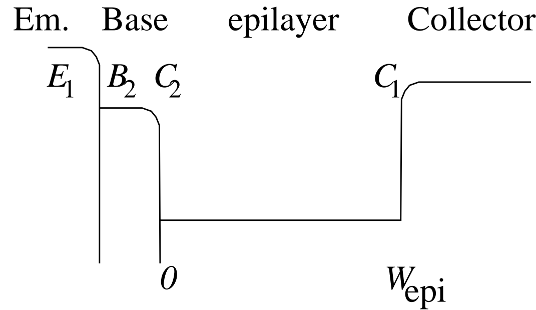

Figure 7: *Schematic representation of the doping profile of a one-dimensional bipolar transistor. One can observe the emitter, the base, the collector epilayer and the (buried) collector. Constant doping profiles are assumed in many of the derivations. The collector epilayer is in this chapter located between* $x = 0$ *and* $x = W_{\mathrm{epi}}$ *and has a dope of* N_{epi}. *We have also shown where the various nodes* E_1, B_2, C_2 *and* C_1 *of the intrinsic transistor are located approximately.*

for instance, depletion charges and capacitances that have a parameter for the grading coefficient, instead of having the ideal grading coefficient of 1/2.) For the same reason most of the parameters will have an effective value. This is even more so when current spreading is taken into account.

We assume that the potential of the buried layer, at the interface with the epilayer, is given by the node potential $\mathcal{V}_{\mathrm{C}_1}$. The resistance in the buried layer and further away at the collector contact are modelled by the resistance R_{Cc} and will not be discussed here.

We assume that the doping concentration in the base is much higher than that in the epilayer. In that case the depletion region will be located almost only in the epilayer (i.e. we have a one-sided pn-junction). The potential of the internal base (i.e. the base potential while neglecting the base resistance) is given by $\mathcal{V}_{\mathrm{B}_2}$.

Velocity saturation The drift velocity of carriers is given by the product of the mobility and the electric field. The mobility of the electrons itself, however, also depends on the electric field. It has a low field value μ_{n0}, such that the low-field drift velocity equals $v = \mu_{n0}\, E$. At high electric fields, however, this velocity saturates. the maximum value given by the saturation velocity v_{sat}. A simple equation that can be used to describe this effect is

$$\mu_n = \frac{\mu_{n0}}{1 + \mu_{n0} E / v_{\mathrm{sat}}}; \qquad v = \mu_n E = \frac{\mu_{n0} E}{1 + \mu_{n0} E / v_{\mathrm{sat}}}. \tag{4.1}$$

As one can see there is a cross-over from $v = \mu_{n0} E$ for small electric fields to $v = v_{\mathrm{sat}}$ for large electric fields. This cross-over happens at the critical electric field defined by

$$E_c = \frac{v_{\mathrm{sat}}}{\mu_{n0}}. \tag{4.2}$$

Typical vales for Si are $v_{\mathrm{sat}} = 1.07 \cdot 10^7\,\mathrm{cm/s}$, $\mu_{n0} = 1.0 \cdot 10^3\,\mathrm{cm^2/Vs}$ and $E_c = 7 \cdot 10^3\,\mathrm{V/cm}$.

 ©Koninklijke Philips Electronics N.V. 2002

The current In normal forward mode electrons move from base to collector, i.e. in positive x-direction. The current density J_{epi} is then negative, due to the negative charge of electrons. The current I_{epi} itself, however, is generally defined as going from collector to emitter, via the base, and is positive in forward mode. We therefore write

$$I_{\mathrm{epi}} = -A_{\mathrm{em}}\, J_{\mathrm{epi}}. \tag{4.3}$$

The electric field As mentioned before, the electric field in the epilayer is important. The basic description of the electric field is the same as that in a simple pn-junction. In the epilayer (of an NPN) it is negative. According to general pn-junction theory, the integral of the electric field from node B_2 to node C_1 equals the applied voltage $\mathcal{V}_{\mathrm{C_1B_2}}$ plus the built-in voltage V_{dC}:

$$-\int_{B_2}^{C_1} E(x)\mathrm{d}x = -\int_{0}^{W_{\mathrm{epi}}} E(x)\mathrm{d}x = \mathcal{V}_{\mathrm{C_1B_2}} + V_{dC}. \tag{4.4}$$

Here we assumed that the electric field in the base and in the highly doped collector drops very fast to zero, such that the contribution to the integral only comes from the region $0 < x < W_{\mathrm{epi}}$.

Equation (4.4) is an important limitation on the electric field. It is in itself not enough to find the electric field. To this end we need Gauss' law

$$\frac{\mathrm{d}E}{\mathrm{d}x} = \frac{\rho}{\varepsilon}. \tag{4.5}$$

Here ρ is the total charge density, given by

$$\rho = q(N_{\mathrm{epi}} - n + p). \tag{4.6}$$

Consider now the electric field in an ohmic region. It is constant and has the value

$$E = \frac{J_{\mathrm{epi}}}{\sigma} = -\frac{I_{\mathrm{epi}}}{\sigma A_{\mathrm{em}}}. \tag{4.7}$$

Here σ is the conductivity. The electric field is negative, as mentioned before. In ohmic regions the electric field is low enough to prevent velocity saturation. The net charge is zero and the number of electrons equals the dope N_{epi}. A negligible number of holes are present. The ohmic resistance of the epilayer can then be calculated and is given by the parameter $R_{Cv} = W_{\mathrm{epi}}/q\mu_n A_{\mathrm{em}} N_{\mathrm{epi}}$.

Next we consider the depletion regions. In these regions the electric field will be high. Hence we can assume that the velocity of electrons is saturated. There will be no holes in these regions either. The electron density however depends on the current density. Since the electron velocity is constant we have $n = |J_{\mathrm{epi}}|/v_{\mathrm{sat}}$. The total net charge is then given by a sum of the dope and the charge density resulting from the current: $\rho = qN_{\mathrm{epi}} - |J_{\mathrm{epi}}|/v_{\mathrm{sat}}$. For the charge density it does not matter whether the current moves forth or back. This gives us

$$\frac{\mathrm{d}E}{\mathrm{d}x} = \frac{qN_{\mathrm{epi}}}{\varepsilon}\left(1 - \frac{I_{\mathrm{epi}}}{I_{hc}}\right), \tag{4.8}$$

©Koninklijke Philips Electronics N.V. 2002

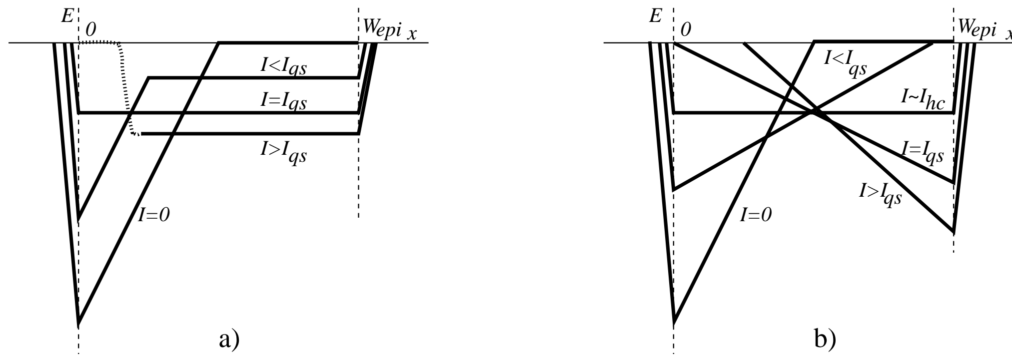

Figure 8: *Figure describing the electric field in the epilayer as function of current. In a) the width of the depletion layer decreases because ohmic voltage drop is the dominant effect. In b) the width of the depletion layer increases because velocity saturation is dominant (Kirk effect). At $I = I_{qs}$ quasi-saturation starts (see text).*

where we defined the hot-carrier current $I_{hc} = q N_{\text{epi}} A_{\text{em}} v_{\text{sat}}$. When the epi-layer current equals the hot-carrier current the total charge in that part of the epilayer will vanish. We still call these regions depleted, since the electrons still move with v_{sat}, in contrast to the ohmic regions.

For currents larger than the hot-carrier current the derivative of the electric field will be negative. There will still be a voltage drop over the epilayer. This voltage drop, however, is no longer ohmic, but space-charge limited. The corresponding resistance of the epilayer is now given by the Space-Charge Resistance SCR_{Cv}. We will discuss this in more detail below.

Let us consider the current dependence of the electric field distribution in some more detail, for both cases discussed above. At low current density (i.e. before quasi-saturation defined below) the electric field in the epilayer is similar to that of a diode in reverse bias. Next to the base we have a depletion region. This region is followed by an ohmic region. When the current increases the width of the depletion layer changes. There are two competing effects that make that this width either increases or decreases, which we will discuss here quantitatively.

We know that the bias over the depletion region itself is given by the bias $\mathcal{V}_{\text{C}_1\text{B}_2}$ minus the ohmic potential drop. Hence when the ohmic region is large the intrinsic junction potential will decrease with current, and so will the depletion region width. This is schematically shown in Fig. 8a). At some point the depletion layer thickness vanishes, and the whole electric field is used for the ohmic voltage drop. Since at higher currents we still need to fulfil Eq. (4.4) the electric field becomes smaller close to the base. This is possible because holes get injected into the epilayer, which reduces the resistance in the region next to the base. This effect, quasi-saturation, will be discussed in more detail later.

The other effect that has an influence on the width of the electric field is velocity saturation. As can be seen from Eq. (4.8), the slope of the electric field decreases with increasing current. This means that to keep the total integral over the electric field constant, as in Eq. (4.4), the width of the depletion layer must increase. This is schematically shown

 ©Koninklijke Philips Electronics N.V. 2002

in Fig. 8b). With increasing current the depletion width will continue to increase, until it reaches the highly doped collector. For even higher currents the total epilayer will be depleted. The slope of the electric field still decreases and can change sign. At some level of current the value of the electric field at the base-epilayer junction drops beneath the critical field E_c for velocity saturation and holes get injected into the epilayer. As before, at this point high injection effects in the epilayer start to play a role. This is again the regime of quasi-saturation. When quasi-saturation is due to a voltage drop as a result of the reversal of the slope of the electric field, the effect is better known as the Kirk effect.

Note that in both cases described above a situation occurs where the electric field is (approximately) flat over the whole epilayer, as shown in Fig. 8. In the ohmic case this will happen at much smaller electric field (and therefore collector-base bias) than in the case of space charge dominated resistance (Kirk effect).

Quasi-saturation Consider the normal forward operating regime. The (external) base collector bias will be negative: $\mathcal{V}_{\mathrm{B_2C_1}} < 0$. The epilayer, however, has some resistance, which can either be ohmic, or space charge limited, as discussed above. As a result the internal base-collector bias, in our model given by $V^*_{B_2C_2}$, is less negative than the external bias. For large enough currents, it even becomes forward biased. This also means that the carrier densities at the base-collector interface increase. At some point, to be more precise when $V^*_{B_2C_2} \simeq \mathsf{V}_{\mathsf{d_C}}$, these carrier densities become comparable to the background doping. From there on high-injection effects in the epilayer become important. This is the regime of quasi-saturation. Note that we use the term quasi-saturation when the voltage drop is due to an ohmic resistance, but also when it is due to a space-charge limited resistance, in which case the effect is also known as Kirk effect.

For our description the current at which quasi-saturation starts, I_{qs}, is very important. So let us consider it in more detail. As mentioned before, quasi-saturation starts when $V^*_{B_2C_2} = \mathsf{V}_{\mathsf{d_C}}$. In that case we can express the integral over the electric field in terms of V_{qs}, the potential drop over the epilayer, using Eq. (4.4):

$$V_{qs} = \mathsf{V}_{\mathsf{d_C}} - \mathcal{V}_{\mathrm{B_2C_1}} = -\int_0^{W_{\mathrm{epi}}} E(x)\mathrm{d}x. \tag{4.9}$$

So, at the onset of quasi-saturation the integral over the electric field is fixed by the external base-collector bias, and does no longer depend on the current. We can then use the relation between the electric field and the current to determine the current I_{qs}. In the ohmic case the electric field is constant over the epilayer. The voltage drop is simply the ohmic voltage drop and we can write

$$I_{qs} = V_{qs}/\mathsf{R_{Cv}}. \tag{4.10}$$

For higher currents the electric field is no longer constant, due to the net charge present in the epilayer. Its derivative is given by Eq. (4.8) and depends on the current. The current at onset of quasi-saturation can still be given as V_{qs} over some effective resistance:

$$I_{qs} = V_{qs}/\mathsf{SCR_{Cv}}. \tag{4.11}$$

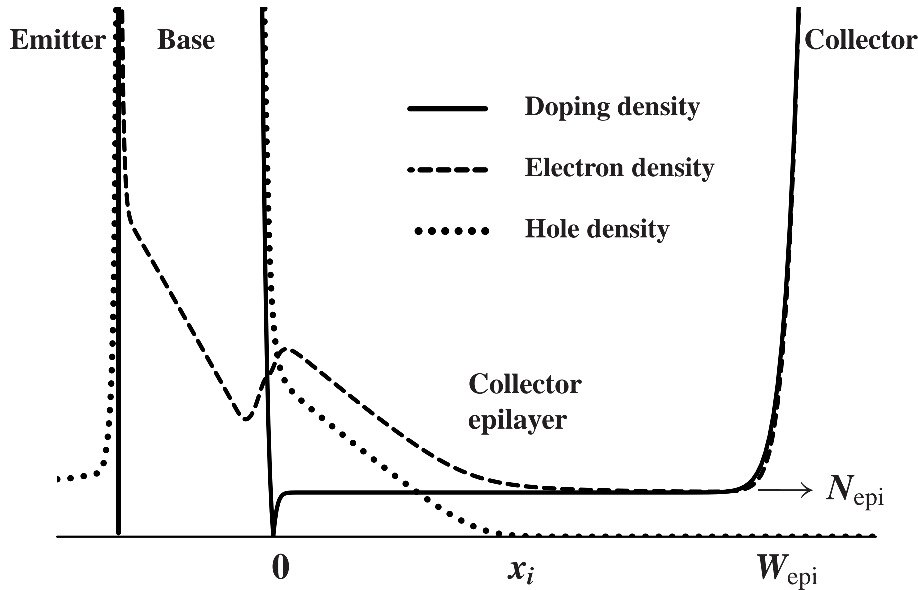

Figure 9: *Schematic view of the doping, electron and hole densities in the base-collector region (on an arbitrary linear scale), in the case of base push-out/quasi-saturation. It also shows the thickness of the epilayer* W_{epi} *and the injection layer* x_i*. From Refs. [17, 18].*

The effective resistance SCR_{Cv} is the space-charge resistance introduced above.

When the (internal) base-collector is forward biased, as in quasi-saturation, holes from the base will be injected in the epilayer. Charge neutrality is maintained in this injection layer, so also the electron density will increase. As we noted already in the description of the main current, at high injection the hole and electron densities will have a linear profile. This linear profile in the base is now continued into the epilayer. The width of the base has effectively become wider, from the base-emitter junction to the end of the injection region in the epilayer. This is known as base push-out and is shown in Fig. 9. It decreases transistor performance considerably. As an example we show the output characteristics in Fig. 10. Note that in the Spice-Gummel-Poon model quasi-saturation is not modelled. The reduction of the current as modelled by Mextram shows the effect.

It is important to note that although the hole density profile and the electron density profile are similar, only the electrons carry current. The electric field and the density gradient work together to move the electrons. However for the holes they act opposite and create an equilibrium. This equilibrium will be used to determine the electric field (which will be considerably below the critical electric field E_c), as is being done in the Kull model. Also the electron current in the injection region will in Mextram be described by the Kull model.

 ©Koninklijke Philips Electronics N.V. 2002

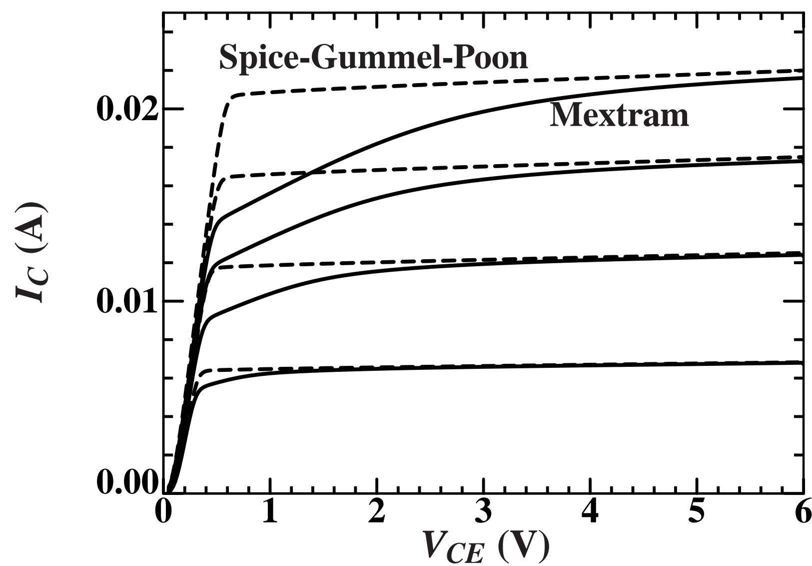

Figure 10: *The output characteristics for both the Spice-Gummel-Poon model and the Mextram model. From Refs. [17, 18].*

©Koninklijke Philips Electronics N.V. 2002

5 The substrate network

Let us consider the substrate under and surrounding the transistor. Mextram models the collector-substrate depletion capacitance. (We will disregard the substrate current here, since it is negligible in normal forward operation.) This means that the Mextram external substrate node is physically located just below the depletion layer in the substrate. This is not the same location as where the substrate is connected to the ground at the level of the interconnect. So there is a physical separation between the Mextram substrate node and the substrate contact. For accurate modelling one needs at least a resistance between the two locations or nodes, as in Fig. 11.

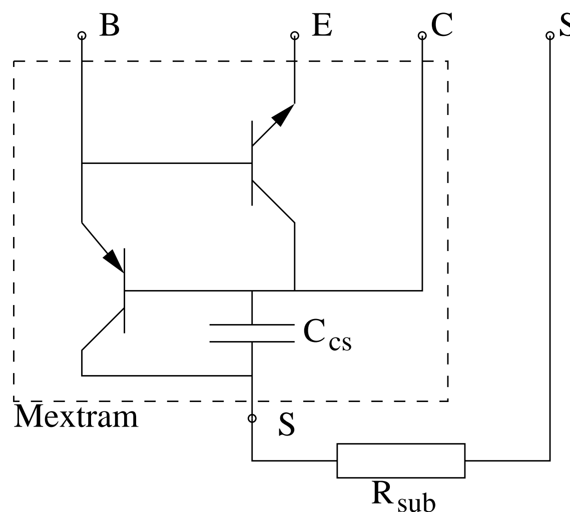

Figure 11: *The most simple substrate network consists of only a resistance between the external Mextram node S and the substrate contact at the top of the wafer.*

Mextram does not have this substrate resistance. Hence one should add it in a macro model. The reason that Mextram does not have this substrate resistance inside the model is related to the fact that this substrate resistance is not known up front. Its actual value depends very much on the location of the substrate plug and substrate contact. Since this location is determined by the designer, at the layout stage, this resistance can also only be determined after the layout is known. Extracting the substrate resistance from on-wafer measurements is possible, but it will not necessarily give the correct value in a real circuit. By having it already as a parameter in the model, the designer will assume it is accurate, which it is not.

There is another reason for not having the substrate resistance within the Mextram model. The distance between the depletion layer of the substrate and the substrate contact is quite large compared to the other transistor dimensions. This also means that at normal operating frequencies non-quasi-static effects can already play a role. The most important contribution to this is probably the charge storage in the AC substrate current path. For this reason one often sees a substrate network as in Fig. 12.

In some cases it is not even accurate to assume a single non-distributed collector-substrate depletion capacitance. In that case an even more elaborate substrate network is needed [19].

 ©Koninklijke Philips Electronics N.V. 2002

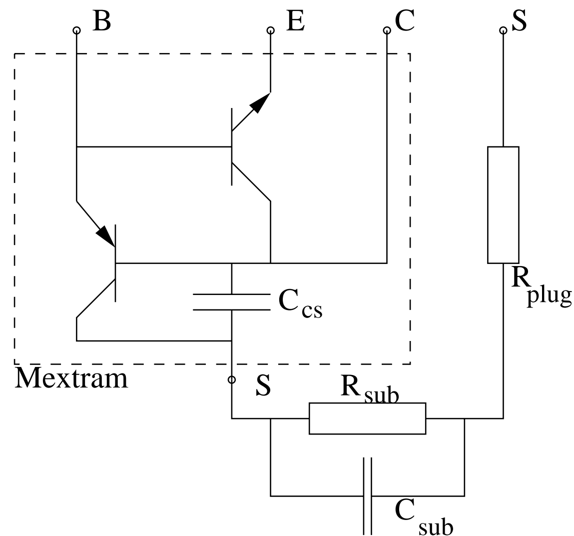

Figure 12: *The more complicated substrate network consists of a resistance* R_{sub} *describing the resistance in the substrate itself, together with its semiconductor capacitance* C_{sub} *and an extra plug/contact resistance* R_{plug}.

So in practice the accuracy needed for the substrate network determines very much how this substrate network should look like. For that reason all of the substrate network is kept outside of Mextram.

©Koninklijke Philips Electronics N.V. 2002

6 Usage of (self)-heating with Mextram

Transistors within a circuit will dissipate power. The generated power has an influence on the temperature of the device and its surroundings. Hence, due to the power dissipation devices in the circuit will get warmer. This is called (self)-heating. In Mextram there are two ways to take this (self)-heating into account. The most direct and well-known way is to include a self-heating network for each transistor and couple these networks to each other via an external thermal network. In this way the heating will be taken into account dynamically. The other way is to estimate the average static temperature increase for each device and use the parameter DTA to increase the temperature of the device. This method is much simpler both in implementation and in circuit simulation than using heating networks. We will discuss both methods below. Note that both methods are *independent* of each other: they do not interact.

6.1 Dynamic heating

Heating can be due to the transistor itself (self-heating) and due to other transistors (mutual heating). Here we discuss the heating if taken into account dynamically.

6.1.1 Self-heating

To describe self-heating we need to consider two things: what is the dissipated power and what is the relation between the dissipated power and the increase in temperature.

Dissipated power The power that flows into a device can be calculated as a sum over currents times voltage drops. For instance for a three-terminal bipolar transistor we can write

$$P = I_C \, \mathcal{V}_{\text{CE}} + I_B \, \mathcal{V}_{\text{BE}}. \tag{6.1}$$

Since normally the collector current is larger than the base current and the collector voltage is larger than the base voltage, the first term is usually dominant.

Not all the power that flows into a transistor will be dissipated. Part of it will be stored as the energy on a capacitor. This part can be released later on. So to calculate the *dissipated* power, we need to add all the contributions of the dissipated elements, i.e., all the DC currents times their voltage drops. We then get

$$P_{\text{diss}} = \sum_{\text{all branches}} I_{\text{branch}} \cdot V_{\text{branch}}. \tag{6.2}$$

The difference between the power flow into the transistor and the dissipated power as calculated above, is stored in the capacitances.

 ©Koninklijke Philips Electronics N.V. 2002

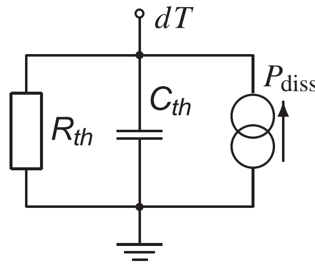

Figure 13: *The self-heating network. Note that for increased flexibility the node dT is made available to the user (see also Fig. 14).*

Relation between power and increase of temperature Next we need a relation between the dissipated power and the rise in temperature. In a DC case we can assume a linear relation: $\Delta T = R_{th}\ P_{\rm diss}$, where the coefficient R_{th} is the thermal resistance (in units K/W). We assume here that it does not matter *where* the power is actually dissipated. In reality, of course, a certain dissipation profile will also give a temperature profile over the transistor: not every part will be equally hot. We will not take this into account.

In non-stationary situations we have to take the finite heat capacity of the device into account [20]. So we must ask ourselves, what happens when a transistor is heated by a small heat source. The dissipated power creates a flow of energy, driven by a temperature gradient, from the transistor to some heat sink far away. The larger the gradient in the temperature, the larger the flow. This means that locally the temperature in the transistor will be larger than in the surrounding material. This increased temperature ΔT is directly related to the increase in the energy ΔU:

$$\Delta U = C_{th}\ \Delta T, \tag{6.3}$$

where C_{th} is the thermal capacitance (or effective heat capacitance) in units J/K. A part of the dissipated power will now flow away, and a part will be used to increase the local energy density if the situation is not yet stationary. Hence we can write

$$P_{\rm diss} = \frac{\Delta T}{R_{th}} + C_{th}\frac{{\rm d}\Delta T}{{\rm d}t}. \tag{6.4}$$

Implementation For the implementation of self-heating an extra network is introduced, see Fig. 13. It contains the thermal resistance R_{th} and capacitance C_{th}, both connected between ground and the temperature node dT. The value of the voltage $\mathcal{V}_{\rm dT}$ at the temperature node gives the increase in local temperature. The power dissipation as given above is implemented as a current source.

©Koninklijke Philips Electronics N.V. 2002

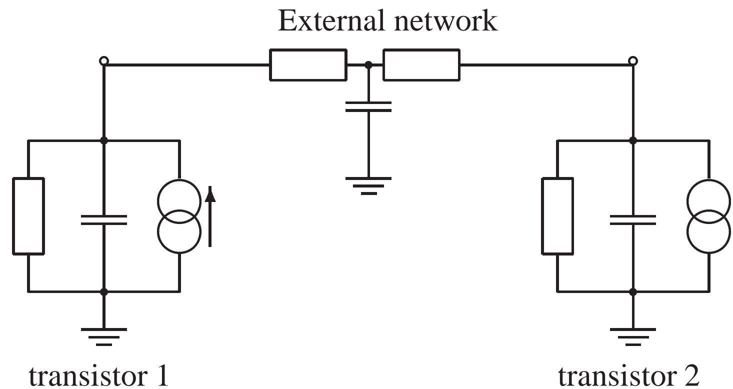

Figure 14: *An example of mutual (and self-) heating of two transistors.*

6.1.2 Mutual heating

Apart from self-heating it is also possible to model mutual heating of two or more transistors close together. To do this the terminals dT of the transistors have to be coupled to each other with an external network. An example is given in Fig. 14. This external network is not an electrical network, but a network of heat-flow and heat-storage (just as the self-heating network within Mextram is not an electrical network). One has to be careful, therefore, not to connect any 'thermal' nodes with 'electrical' nodes. The external network can be made as complicated as one wishes, thermally connecting any number of transistors. For more information we refer to literature, e.g. Refs. [21, 22, 23].

6.1.3 Advantages

The advantages of this method are that heating is taken into account dynamically. Hence the temperature increase of a certain device depends on the actual power dissipation of the device itself, as well as of its surroundings. Any time delays are also taken into account.

6.1.4 Disadvantages

There are a number of disadvantages. First of all, to be able to have an accurate description of the temperature increase of a device one needs to have an accurate thermal network. This means that one needs a lot of thermal resistances and thermal capacitances to give an accurate result. In a sense, one must discretise the heat equations to get a good three-dimensional heat flow. It is not easy to determine all these resistances and capacitances. It is even not easy to determine the self-heating resistance of a single device in its circuit surroundings, which differs from the surroundings in an on-wafer extraction module.

One of the other disadvantages has to do with the difference of time scale between heating effects (of the order of 1 µs or slower depending on the distance) and the time scale of electronic signals (often of the order of 1 ns or less). This can cause difficulties in simulations. It takes many signal cycles to generate a good number for the average power dissipation.

 ©Koninklijke Philips Electronics N.V. 2002

Another important disadvantage is the extra increase in complexity and hence simulation time. First of all, the extra thermal network has to be simulated. But this will, in practice not be too bad. Then for all devices one must take into account all the derivatives w.r.t. temperature. This takes extra time. And then the addition of self-heating makes the convergence process of the simulation more difficult. It will therefore take more time. And for difficult circuits (in the simulation sense) convergence might not even be reached.

6.2 Static heating

In practice it is often not necessary to take self-heating into account dynamically. Often the circuit will have an average dissipation. This dissipation will generate a certain temperature profile over the circuit. For instance, a power intensive circuit will be hotter than its surroundings. Changes in this temperature profile are much slower than the time-scales on which the circuit operates. Only the time-averaged power dissipation is then relevant.

For these cases Mextram (and other Philips models) have an extra parameter *DTA*. This parameter is used to increase the local ambient temperature w.r.t. the global ambient temperature. It is very useful for giving a part of the circuit an increased temperature. Since many complex designs contain various circuit blocks, it is indeed quite handy to be able to give the more power-intensive blocks a larger local ambient temperature. This feature of using *DTA* to increase the local temperature can also be used for more complex situations, where for instance the temperature has a gradient. This can occur, for instance, close to a power-intensive circuit block.

6.2.1 Advantages

The method is very fast. Once the temperature profile is given and the parameters *DTA* are set, the simulation does not take more time than a simulation which does not include heating. Instances of Mextram transistors without self-heating (and hence without the self-heating node) can be used.

6.2.2 Disadvantages

The method is less accurate. The increase in temperature depending on whether a transistor is on or not is not taken into account.

Of course one must have a method to estimate the temperature profiles. This is not always easy. On the other hand, it is probably easier than making a complete thermal network.

6.3 Combining static and dynamic heating

As discussed above, there are two methods for increasing the temperature of the device. The easiest method is using the parameter *DTA* to give a static heating. This increases the

local ambient temperature:

$$T_{\text{local ambient}} = T_{\text{global ambient}} + \mathit{DTA}. \tag{6.5}$$

Apart from that, it is also possible to take dynamic heating into account, using the self-heating network, possibly connected to an external thermal network to give mutual heating. The device temperature is then given by

$$T_{\text{device}} = T_{\text{local ambient}} + (\Delta T)_{\text{dynamic heating}}. \tag{6.6}$$

It is important to realise that within Mextram these two ways of heating the transistor are independent and that the temperature increases are additive. An increase using DTA therefore does *not* generate a heat-flow through a thermal network.

It is perfectly possible to take self- and mutual heating of two critical transistors into account, even if both have a, possibly different, local ambient temperature increase. Consider for instance the following situation. We have two transistors close together, like in Fig. 14. One of them is also heated statically by a nearby part of the circuit and therefore has some $\mathit{DTA} > 0$. We assume that the second transistor is further away from this heat-source. In that case the second transistor will be heated both by the static heat-source, as well as by the first transistor. For the heating by the first transistor the thermal network as in Fig. 14 takes care. In principle this same thermal network could be used to model the heat flow due to the static heat-source from the first transistor to the second transistor. In Mextram the parameter DTA does, however, not increase the value of ΔT at the thermal node of the first transistor (because static and dynamic heating are independent). An increased DTA at the first transistor therefore does not generate a heat-flow to the second transistor. So the thermal network can not be used in conjunction with a static increase via DTA. It is important to realise that this is not a mistake in the model. In some sense it is even more physical, as we will show below. Interaction between both ways of heating is not even needed. The independence between static and dynamic heating is therefore rather a feature than a short-coming.

So let us consider the physical behaviour. The heat from the static heat-source is actually not flowing to the first transistor, and from there on to the second transistor. It is flowing from the source in all directions and generates a static temperature distribution. It can flow around the first transistor. The value of the resulting temperature increase at the location of the second transistor is the value that must be given to the DTA of this second transistor. In this way not only the effects of heating by a static heat-source and dynamic heating via a thermal network are independently added, also the thermal behaviour of both heat-flows can be taken to be independent. For modelling two nearby transistors a very simple thermal network, as in Fig. 14 is enough. This simple thermal network is, however, insufficient to describe the heat-flow from the static source. For the static source, on the other hand, one does not need to make such a thermal network, since only the temperature profile is important.

Furthermore, it is not even necessary to take the static heating into account via a thermal network. Once the thermal network is given, and once the temperature (or power dissipation) of the static source is know, the increase of temperature at each transistor in the

 ©Koninklijke Philips Electronics N.V. 2002

thermal network due solely to the static source can be calculated up front. The parameter *DTA* can be used for this temperature increase. Any dynamic heating is then added by the simulator. The only assumption in this is that the dynamic heating does not influence the heat-flow due to the static source. The possible errors made by this assumption are far less then the errors made by the lack of knowledge about actual temperature profiles or heat flow.

6.4 The thermal capacitance

The reason for having a thermal capacitance was already explained above. In practice the thermal capacitance is often not very important. For DC simulations is has no influence at all. For RF simulations the delay time of the self-heating is so long that only the average dissipated power is important, and not the instantaneous. The frequencies where the thermal capacitance becomes important are around 1 MHz.

When you look at the small signal parameters of the transistor, for instance the output conductance, then you see a change as function of frequency. For a SiGe transistor, for instance, the collector current at fixed base current will decrease as function of collector voltage due to self-heating. This means that the low-frequency output conductance is negative. At very high frequencies self-heating has no influence on the output conductance, and it will be positive. As function of frequency one will therefore observe a change from negative values to positive values. In the case of pure Si transistors the output conductance will not be negative at low currents, but still one can see a transition.

Although the exact value of the thermal capacitance is often not important for simulations, it is *not* good to give it a value of 0, say as a default in a parameter set. The reason for this is that the RF simulations will give a wrong result (effectively, as if it were low-frequency simulations).

©Koninklijke Philips Electronics N.V. 2002

7 Operating point information

The operating point information is a list of quantities that describe the internal state of the transistor. When a circuit simulator is able to provide these, it might help the designer understand the behaviour of the transistor and the circuit.

The full list of operating point information consists of three parts. First all the branch biases, the currents and the charges are present. Then there are the elements that can be used if a full small-signal equivalent circuit is needed. These are all the derivatives of the charges and currents. At last, and this is the most informative for a designer, the operating point information gives usable approximations for use in a hybrid-π model. This hybrid-π model is the basic model used by many designers for hand-calculations. It should give similar results as Mextram, as long as neither the current, nor the frequency are too high. In addition also the cut-off frequency is included in the operating point information.

7.1 Approximate small-signal circuit

In our presentation, we will start with the hybrid-π model. The approximate small-signal model is shown Fig. 15. This model contains the following elements that can be found from in operating point information (for the derivation of these various quantities, we refer to Ref. [11]):

g_m	Transconductance
β	Current amplification
g_{out}	Output conductance
g_μ	Feedback transconductance
R_E	Emitter resistance
r_B	Base resistance
R_{Cc}	Constant collector resistance
C_{BE}	Base-emitter capacitance
C_{BC}	Base-collector capacitance
C_{ts}	Collector-substrate capacitance

As mentioned before, one can also find the cut-off frequency of the transistor in the operating point information. The approximation for f_T is much more accurate than can be found from the equivalent circuit above.

f_T	Good approximation for cut-off frequency

Related to self-heating, the dissipation and actual temperature are also available

$P_{\rm diss}$	Dissipation
T_K	Actual temperature

Then there are a few extra quantities available for the experienced user:

I_{qs}	Current at onset of quasi-saturation
$x_i\,/\,W_{\rm epi}$	Thickness of injection layer
$V^*_{B_2C_2}$	Physical value of internal base-collector bias

 ©Koninklijke Philips Electronics N.V. 2002

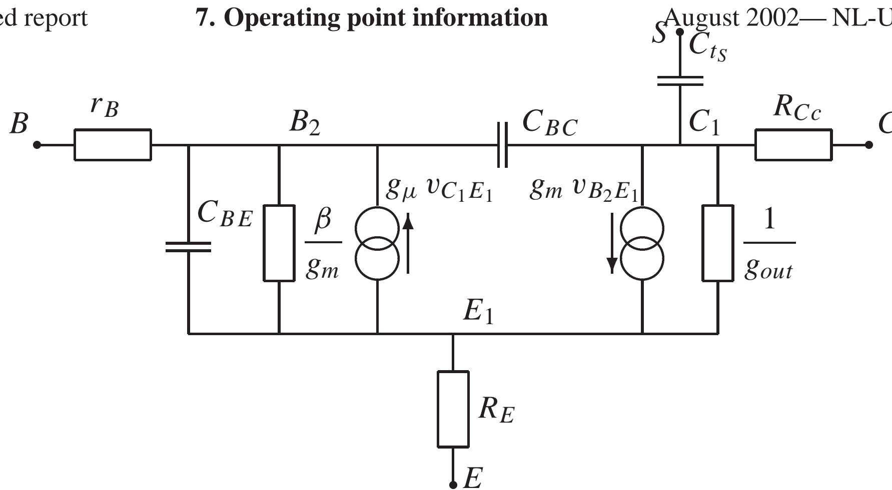

Figure 15: *Small-signal equivalent circuit describing the approximate behaviour of the Mextram model. The actual forward Early voltage can be found as* $V_{eaf} = I_C/g_{out} - \mathcal{V}_{\mathrm{CE}}$. *which can be different from the parameter value* V_{ef}*, especially when* $dE_g \neq 0$.

7.2 DC currents and charges

In this section the biases, DC currents and charges are listed.

Since we have 5 internal nodes we need 5 voltage differences to describe the bias at each internal node, given the external biases. We take those that are the most informative for the internal state of the transistor:

$\mathcal{V}_{\mathrm{B_2E_1}}$	Internal base-emitter bias
$\mathcal{V}_{\mathrm{B_2C_2}}$	Internal base-collector bias
$\mathcal{V}_{\mathrm{B_2C_1}}$	Internal base-collector bias including epilayer
$\mathcal{V}_{\mathrm{B_1C_1}}$	External base-collector bias without contact resistances
$\mathcal{V}_{\mathrm{E_1E}}$	Bias over emitter resistance

The actual currents (and charges, see next page) are:

I_N	Main current
$I_{C_1C_2}$	Epilayer current
$I_{B_1B_2}$	Pinched-base current
I_{B_1}	Ideal forward base current
$I_{B_1}^S$	Ideal side-wall base current
I_{B_2}	Non-ideal forward base current
I_{B_3}	Non-ideal reverse base current
I_{sub}	Substrate current
I_{avl}	Avalanche current
I_{ex}	Extrinsic reverse base current
XI_{ex}	Extrinsic reverse base current
XI_{sub}	Substrate current
I_{Sf}	Substrate failure current
I_{R_E}	Current through emitter resistance
$I_{R_{Bc}}$	Current through constant base resistance
$I_{R_{Cc}}$	Current through constant collector resistance

Q_E	Emitter charge or emitter neutral charge
Q_{t_E}	Base-emitter depletion charge
$Q_{t_E}^S$	Sidewall base-emitter depletion charge
Q_{BE}	Base-emitter diffusion charge
Q_{BC}	Base-collector diffusion charge
Q_{t_C}	Base-collector depletion charge
Q_{epi}	Epilayer diffusion charge
$Q_{B_1B_2}$	AC current crowding charge
Q_{tex}	Extrinsic base-collector depletion charge
XQ_{tex}	Extrinsic base-collector depletion charge
Q_{ex}	Extrinsic base-collector diffusion charge
XQ_{ex}	Extrinsic base-collector diffusion charge
Q_{t_S}	Collector-substrate depletion charge

7.3 Elements of full small-signal circuit

The small-signal equivalent circuit contains the following conductances. In the terminology we use the notation A_x, A_y, and A_z to denote derivatives of the quantity A to some voltage difference. We use x for base-emitter biases, y is for derivatives w.r.t. $\mathcal{V}_{\mathrm{B_2C_2}}$ and z is used for all other base-collector biases. The subindex π is used for base-emitter base currents, μ is used for base-collector base currents, Rbv for derivatives of $I_{B_1B_2}$ and Rcv for derivatives of $I_{C_1C_2}$.

(See next page)

 ©Koninklijke Philips Electronics N.V. 2002

Quantity	Equation	Description
g_x	$\partial I_N / \partial \mathcal{V}_{\mathrm{B_2E_1}}$	Forward transconductance
g_y	$\partial I_N / \partial \mathcal{V}_{\mathrm{B_2C_2}}$	Reverse transconductance
g_z	$\partial I_N / \partial \mathcal{V}_{\mathrm{B_2C_1}}$	Reverse transconductance
g_π^S	$\partial I_{B_1}^S / \partial \mathcal{V}_{\mathrm{B_1E_1}}$	Conductance sidewall b-e junction
$g_{\pi,x}$	$\partial (I_{B_1} + I_{B_2}) / \partial \mathcal{V}_{\mathrm{B_2E_1}}$	Conductance floor b-e junction
$g_{\pi,y}$	$\partial I_{B_1} / \partial \mathcal{V}_{\mathrm{B_2C_2}}$	Early effect on recombination base current
$g_{\pi,z}$	$\partial I_{B_1} / \partial \mathcal{V}_{\mathrm{B_2C_1}}$	Early effect on recombination base current
$g_{\mu,x}$	$-\partial I_{\mathrm{avl}} / \partial \mathcal{V}_{\mathrm{B_2E_1}}$	Early effect on avalanche current limiting
$g_{\mu,y}$	$-\partial I_{\mathrm{avl}} / \partial \mathcal{V}_{\mathrm{B_2C_2}}$	Conductance of avalanche current
$g_{\mu,z}$	$-\partial I_{\mathrm{avl}} / \partial \mathcal{V}_{\mathrm{B_2C_1}}$	Conductance of avalanche current
$g_{\mu\mathrm{ex}}$	$\partial (I_{\mathrm{ex}} + I_{B_3} / \partial \mathcal{V}_{\mathrm{B_1C_1}}$	Conductance extrinsic b-c junction
$Xg_{\mu\mathrm{ex}}$	$\partial XI_{\mathrm{ex}} / \partial \mathcal{V}_{\mathrm{BC_1}}$	Conductance extrinsic b-c junction
$g_{Rcv,y}$	$\partial I_{C_1C_2} / \partial \mathcal{V}_{\mathrm{B_2C_2}}$	Conductance of epilayer current
$g_{Rcv,z}$	$\partial I_{C_1C_2} / \partial \mathcal{V}_{\mathrm{B_2C_1}}$	Conductance of epilayer current
r_{bv}	$1/(\partial I_{B_1B_2} / \partial \mathcal{V}_{\mathrm{B_1B_2}})$	Base resistance
$g_{Rbv,x}$	$\partial I_{B_1B_2} / \partial \mathcal{V}_{\mathrm{B_2E_1}}$	Early effect on base resistance
$g_{Rbv,y}$	$\partial I_{B_1B_2} / \partial \mathcal{V}_{\mathrm{B_2C_2}}$	Early effect on base resistance
$g_{Rbv,z}$	$\partial I_{B_1B_2} / \partial \mathcal{V}_{\mathrm{B_2C_1}}$	Early effect on base resistance
R_E	R_{ET}	Emitter resistance (already given above)
R_{Bc}	R_{BcT}	Constant base resistance
R_{Cc}	R_{CcT}	Constant collector resistance (already given above)
g_S	$\partial I_{\mathrm{sub}} / \partial \mathcal{V}_{\mathrm{B_1C_1}}$	Conductance parasitic PNP transistor
Xg_S	$\partial XI_{\mathrm{sub}} / \partial \mathcal{V}_{\mathrm{BC_1}}$	Conductance parasitic PNP transistor
g_{Sf}	$\partial I_{\mathrm{Sf}} / \partial \mathcal{V}_{\mathrm{SC_1}}$	Conductance substrate failure current

The small-signal equivalent circuit contains the following capacitances

Quantity	Equation	Description
C_{BE}^S	$\partial Q_{t_E}^S / \partial \mathcal{V}_{\mathrm{B_1E_1}}$	Capacitance sidewall b-e junction
$C_{BE,x}$	$\partial (Q_{t_E} + Q_{BE} + Q_E) / \partial \mathcal{V}_{\mathrm{B_2E_1}}$	Capacitance floor b-e junction
$C_{BE,y}$	$\partial Q_{BE} / \partial \mathcal{V}_{\mathrm{B_2C_2}}$	Early effect on b-e diffusion charge
$C_{BE,z}$	$\partial Q_{BE} / \partial \mathcal{V}_{\mathrm{B_2C_1}}$	Early effect on b-e diffusion charge
$C_{BC,x}$	$\partial Q_{BC} / \partial \mathcal{V}_{\mathrm{B_2E_1}}$	Early effect on b-c diffusion charge
$C_{BC,y}$	$\partial (Q_{t_C} + Q_{BC} + Q_{\mathrm{epi}}) / \partial \mathcal{V}_{\mathrm{B_2C_2}}$	Capacitance floor b-c junction
$C_{BC,z}$	$\partial (Q_{t_C} + Q_{BC} + Q_{\mathrm{epi}}) / \partial \mathcal{V}_{\mathrm{B_2C_1}}$	Capacitance floor b-c junction
$C_{BC\mathrm{ex}}$	$\partial (Q_{\mathrm{tex}} + Q_{\mathrm{ex}}) / \partial \mathcal{V}_{\mathrm{B_1C_1}}$	Capacitance extrinsic b-c junction
$XC_{BC\mathrm{ex}}$	$\partial (XQ_{\mathrm{tex}} + XQ_{\mathrm{ex}}) / \partial \mathcal{V}_{\mathrm{BC_1}}$	Capacitance extrinsic b-c junction
$C_{B_1B_2}$	$\partial Q_{B_1B_2} / \partial \mathcal{V}_{\mathrm{B_1B_2}}$	Capacitance AC current crowding
$C_{B_1B_2,x}$	$\partial Q_{B_1B_2} / \partial \mathcal{V}_{\mathrm{B_2E_1}}$	Cross-capacitance AC current crowding
$C_{B_1B_2,y}$	$\partial Q_{B_1B_2} / \partial \mathcal{V}_{\mathrm{B_2C_2}}$	Cross-capacitance AC current crowding
$C_{B_1B_2,z}$	$\partial Q_{B_1B_2} / \partial \mathcal{V}_{\mathrm{B_2C_1}}$	Cross-capacitance AC current crowding
C_{t_S}	$\partial Q_{t_S} / \partial \mathcal{V}_{\mathrm{SC_1}}$	Capacitance s-c junction (already given above)

©Koninklijke Philips Electronics N.V. 2002

 ©Koninklijke Philips Electronics N.V. 2002

References

[1] For the most recent model descriptions, source code, and documentation, see the web-site http://www.semiconductors.philips.com/Philips_Models.

[2] J. C. J. Paasschens and W. J. Kloosterman, "The Mextram bipolar transistor model, level 504," Unclassified Report NL-UR 2000/811, Philips Nat.Lab., 2000. See Ref. [1].

[3] J. J. Ebers and J. L. Moll, "Large signal behaviour of junction transistors," *Proc. IRE*, vol. 42, p. 1761, 1954.

[4] H. K. Gummel and H. C. Poon, "An integral charge control model of bipolar transistors," *Bell Sys. Techn. J.*, vol. May-June, pp. 827–852, 1970.

[5] R. S. Muller and T. I. Kamins, *Device electronics for integrated circuits*. Wiley, New York, 2nd ed., 1986.

[6] S. M. Sze, *Physics of Semiconductor Devices*. Wiley, New York, 2nd ed., 1981.

[7] I. E. Getreu, *Modeling the bipolar transistor*. Elsevier Sc. Publ. Comp., Amsterdam, 1978.

[8] H. C. de Graaff and F. M. Klaassen, *Compact transistor modelling for circuit design*. Springer-Verlag, Wien, 1990.

[9] J. Berkner, *Kompaktmodelle für Bipolartransistoren. Praxis der Modellierung, Messung und Parameterbestimmung — SGP, VBIC, HICUM und MEXTRAM (Compact models for bipolar transistors. Practice of modelling, measurement and parameter extraction — SGP, VBIC, HICUM und MEXTRAM)*. Expert Verlag, Renningen, 2002. (In German).

[10] P. A. H. Hart, *Bipolar and bipolar-mos integration*. Elsevier, Amsterdam, 1994.

[11] J. C. J. Paasschens, W. J. Kloosterman, and R. van der Toorn, "Model derivation of Mextram 504. The physics behind the model," Unclassified Report NL-UR 2002/806, Philips Nat.Lab., 2002. See Ref. [1].

[12] J. C. J. Paasschens, W. J. Kloosterman, and R. J. Havens, "Parameter extraction for the bipolar transistor model Mextram, level 504," Unclassified Report NL-UR 2001/801, Philips Nat.Lab., 2001. See Ref. [1].

[13] H. K. Gummel, "A charge control relation for bipolar transistors," *Bell Sys. Techn. J.*, vol. January, pp. 115–120, 1970.

[14] J. C. J. Paasschens, W. J. Kloosterman, and R. J. Havens, "Modelling two SiGe HBT specific features for circuit simulation," in *Proc. of the Bipolar Circuits and Technology Meeting*, pp. 38–41, 2001. Paper 2.2.

©Koninklijke Philips Electronics N.V. 2002

[15] J. R. Hauser, "The effects of distributed base potential on emitter-current injection density and effective base resistance for stripe transistor geometries," *IEEE Trans. Elec. Dev.*, vol. May, pp. 238–242, 1964.

[16] H. Groendijk, "Modeling base crowding in a bipolar transistor," *IEEE Trans. Elec. Dev.*, vol. ED-20, pp. 329–330, 1973.

[17] J. C. J. Paasschens, W. J. Kloosterman, R. J. Havens, and H. C. de Graaff, "Improved compact modeling of ouput conductance and cutoff frequency of bipolar transistors," *IEEE J. of Solid-State Circuits*, vol. 36, pp. 1390–1398, 2001.

[18] J. C. J. Paasschens, W. J. Kloosterman, R. J. Havens, and H. C. de Graaff, "Improved modeling of ouput conductance and cut-off frequency of bipolar transistors," in *Proc. of the Bipolar Circuits and Technology Meeting*, pp. 62–65, 2000. Paper 3.3.

[19] S. D. Harker, R. J. Havens, J. C. J. Paasschens, D. Szmyd, L. F. Tiemeijer, and E. F. Weagel, "An S-parameter technique for substrate resistance characterization of RF bipolar transistors," in *Proc. of the Bipolar Circuits and Technology Meeting*, pp. 176–179, 2000. Paper 10.2.

[20] C. Kittel and H. Kroemer, *Thermal Physics*. Freeman & Co., second ed., 1980.

[21] J. S. Brodsky, R. M. Fox, and D. T. Zweidinger, "A physics-based dynamic thermal impedance model for vertical bipolar transistors on soi substrates," *IEEE Trans. Elec. Dev.*, vol. 46, pp. 2333–2339, 1999.

[22] P. Palestri, A. Pacelli, and M. Mastrapasqua, "Thermal resistance in $Si_{1-x}Ge_x$ HBTs on bulk-Si and SOI substrates," in *Proc. of the Bipolar Circuits and Technology Meeting*, pp. 98–101, 2001. Paper 6.1.

[23] D. J. Walkey, T. J. Smy, R. G. Dickson, J. S. Brodsky, D. T. Zweidinger, and R. M. Fox, "A VCVS-based equivalent circuit model for static substrate thermal coupling," in *Proc. of the Bipolar Circuits and Technology Meeting*, pp. 102–105, 2001. Paper 6.2.

 ©Koninklijke Philips Electronics N.V. 2002